JOURNAL OF PETROLOGY | VOLUME 41 | NUMBER 8 | PAGES 1307–1327 | 2000

Metamorphism and Anatexis in the Mafic Complex Contact Aureole, Ivrea Zone, Northern Italy

SCOTT A. BARBOZA* AND GEORGE W. BERGANTZ

UNIVERSITY OF WASHINGTON, DEPARTMENT OF GEOLOGICAL SCIENCES, SEATTLE, WA 98195, USA

RECEIVED APRIL 16, 1999; REVISED TYPESCRIPT ACCEPTED JANUARY 14, 2000

Emplacement of mantle-derived magma (magmatic accretion) is often presumed or inferred to be an important cause of regional granulite facies metamorphism and crustal anatexis. The juxtaposition of mafic cumulates and regionally distributed granulite facies rocks has led some to consider the Ivrea zone (northern Italy, Southern Alps) as an important exposure that demonstrates this causal relationship. However, regional PTt *paths indicated by metamorphic reaction textures and* PT *conditions inferred from geothermobarometry indicate that the emplacement of mafic plutonic rocks (Mafic Complex) at the Ivrea zone occurred during decompression from ambient pressures at the regional thermal maximum. Field and petrographic observations, supported by* PT *estimates, indicate that regional retrograde decompression and emplacement of the upper parts of the Mafic Complex probably accompanied extension during the Late Carboniferous–Early Permian. A spatially restricted decompression-melting event accompanied final emplacement, depleting supracrustal rocks enclosed by an* ~*2–3 km aureole overlying the upper Mafic Complex by 20–30% granite component. The upper Mafic Complex provided the thermal energy to reset mineral assemblages and locally overprint the regional prograde metamorphic zonation. The limited extent of the contact aureole suggests that magmatic accretion may not inexorably cause regional metamorphism and crustal anatexis.*

KEY WORDS: *Granulite facies; Ivrea zone; underplating; thermobarometry; migmatite; mafic complex*

INTRODUCTION

The accretion of mantle-derived magma at or near the base of the crust (Wells, 1980; Bohlen, 1987) can enhance the total thermal budget of the continental lower crust, produce regional granulite facies metamorphism, and generate Y- and heavy rare earth element (HREE)-depleted granitoids (Ellis, 1987). Accretion of mafic magma and migration of partial melt will internally stratify, chemically differentiate, and deplete the continental lower crust in large ion lithophile elements (LILE). Magmatic accretion has been invoked to provide the heat and mass necessary for sustained magmatism in tectonic settings such as Phanerozoic extensional terranes (Lister *et al.*, 1986; Gans, 1987; Fountain, 1989; Mareschal & Bergantz, 1990; Jarchow *et al.*, 1993) and magmatic arcs (Hamilton, 1981; Kay & Kay, 1981; Bohlen & Lindsley, 1987; Hildreth & Moorbath, 1988).

However, as few exposed sections of lower continental crust show contiguous mafic intrusions and regionally distributed granulite facies rocks, estimates of the extent of anatexis and metamorphism accompanying magmatic accretion have relied on numerical and analog simulations. These models yield disparate results depending on whether heat transfer within the mafic intrusion and surrounding country rocks is primarily convective (Campbell & Turner, 1987; Huppert & Sparks, 1988) or conductive (Marsh, 1989; Bergantz & Dawes, 1994; Barboza & Bergantz, 1996). A comparison with field evidence is required to discriminate between the model results. In the Ivrea zone, an exposed section of mafic plutonic rocks (the Mafic Complex) has been interpreted to represent deformed cumulates of the accreted magmas that caused regional granulite facies metamorphism (Rivalenti *et al.*, 1975, 1980; Schmid & Wood, 1976; Sills, 1984; Pin, 1990). The continuous exposure between granulite facies crustal rocks and the mafic intrusion that

*Corresponding author. Present address: ExxonMobil Upstream Research Company, Hydrocarbon Systems Analysis Division, PO Box 2189, Houston, TX 77252-2189, USA. Telephone: +1-(713)431-7357. Fax: +1-(713)431-7265. e-mail: scott.a.barboza@exxon.sprint.com

is thought to have provided the heat during regional metamorphism has led some to consider the Ivrea zone a particularly important example of magmatic accretion (e.g. Voshage *et al.*, 1990).

However, Barboza *et al.* (1999) provided field and geochemical data supporting an alternative model (Zingg *et al.*, 1990; Schmid, 1993), in which regional granulite facies metamorphism preceded the emplacement of the upper parts of the Mafic Complex. In this paper, we present whole-rock major- and trace-element compositional data, an inferred sequence of metamorphic reactions, and *PT* estimates derived from thermobarometry for supracrustal rocks proximal to the Mafic Complex. These new data suggest that the emplacement of a major part of the Mafic Complex occurred during decompression from ambient pressures at the thermal maximum during the regional granulite facies episode. Final emplacement caused anatexis and metamorphism only within a narrow ($\sim$2–3 km) aureole in the proximal supracrustal rocks. These events overprint the regional amphibolite to granulite facies prograde metamorphic zonation.

GEOLOGICAL SETTING

Regional framework

The Ivrea zone is one of three fault-bounded sections of Paleozoic basement exposed in the Southern Alps. From the originally deepest to shallowest crustal levels, the Paleozoic Southern Alpine crust comprises the Ivrea, Strona–Ceneri (or Serie dei Laghi in the Italian literature), and Val Colla zones. To the north and west, the Ivrea zone (Fig. 1) is separated from rocks of the Penninic belt by the Insubric Line, a major, NW-dipping, Neogene shear zone that juxtaposes pre-Alpine and Alpine structures and rocks (Gansser, 1968; Schmid *et al.*, 1987). To the south and east, the Cremosina, Cossato–Mergozzo–Brissago (CMB), and the Pogallo Lines separate the Ivrea zone from plutonic rocks and amphibolite facies orthogneiss and paragneiss of the Strona–Ceneri zone (Boriani & Sacchi, 1973; Boriani *et al.*, 1977, 1990*a*; Hodges & Fountain, 1984; Handy, 1987; Schmid *et al.*, 1987).

Most regional studies have interpreted the Ivrea zone as a cross-section through attenuated lower continental crust (Fountain, 1976; Burke & Fountain, 1990). This interpretation is based on gravity and seismic studies that indicate the Ivrea zone is the surface expression of a large, high-density body (the Ivrea geophysical body) situated where the fossilized (pre-Alpine) Southern Alpine Moho comes closest to the surface (Mueller *et al.*, 1980; Giese *et al.*, 1982). Geophysical modeling suggests that the Ivrea body may be a NNE-striking, SE-dipping sliver of Southern Alpine crust and mantle juxtaposed against Austroalpine and Penninic crustal rocks to the north and west (Berckhemer, 1968; Giese *et al.*, 1982; Hirn *et al.*, 1989). This geophysical model is consistent with structural data indicating that steep tilting accompanied emplacement during Alpine collision and closure of the Tethys (Schmid *et al.*, 1987; Nicolas *et al.*, 1990). The mafic plutonic rocks exposed along the Insubric Line (the Mafic Complex) represent the originally deepest levels of exposed crust, and the shallowest levels are represented by supracrustal rocks (the Kinzigite Formation) juxtaposed with the Strona–Ceneri zone (Fig. 1). Although alternative interpretations have been proposed (see Boriani *et al.*, 1990*b*), steep tilting of the Ivrea zone is supported by the regional increase in metamorphic grade to the NW (Schmid, 1967; Mehnert, 1975; Zingg, 1980) and the regional baric gradient according to thermobarometry (Sills, 1984; Henk *et al.*, 1997; Demarchi *et al.*, 1998).

ROCK TYPES

Mafic Complex

The Mafic Complex, commonly interpreted to have been the heat source for regional metamorphism, consists of mafic plutonic rocks and mantle peridotite that form a belt spanning the length of the Ivrea zone along its western and northwestern margin. For the purpose of this study, we make an important distinction between the upper and lower parts of the Mafic Complex. Upper Val Grande and Val d'Ossola expose several hundred meters to 1 km thickness of banded pyroxene–hornblende and hornblende granofels ('pyribolite'; Schmid, 1967). Similar rocks are exposed in upper Val Sesia and Val Strona di Omegna (Mehnert, 1975; Rivalenti *et al.*, 1975). On the basis of field relationships (Quick *et al.*, 1994), compositional trends (Sinigoi *et al.*, 1994), and microstructures, J. E. Quick (personal communication, 1999) suggested that these rocks may be related and represent a phase of magmatism earlier than that of the upper Mafic Complex. These rocks may have been derived from a compositionally distinct parent magma and have undergone a different deformational history from the upper Mafic Complex (Rivalenti *et al.*, 1975; Zingg *et al.*, 1990). Therefore, we distinguish these rocks (referred to collectively hereafter as the lower Mafic Complex) from the overlying deformed cumulates of the upper Mafic Complex (Fig. 1). As the field relationships between the lower Mafic Complex and the overlying supracrustal sections are obscured by the (possibly) younger phase of magmatism, we confine our interpretations to the timing of regional granulite facies metamorphism and emplacement of the upper Mafic Complex.

We focus our study on the southern Ivrea zone (Fig. 1) where the Mafic Complex reaches its maximum exposed

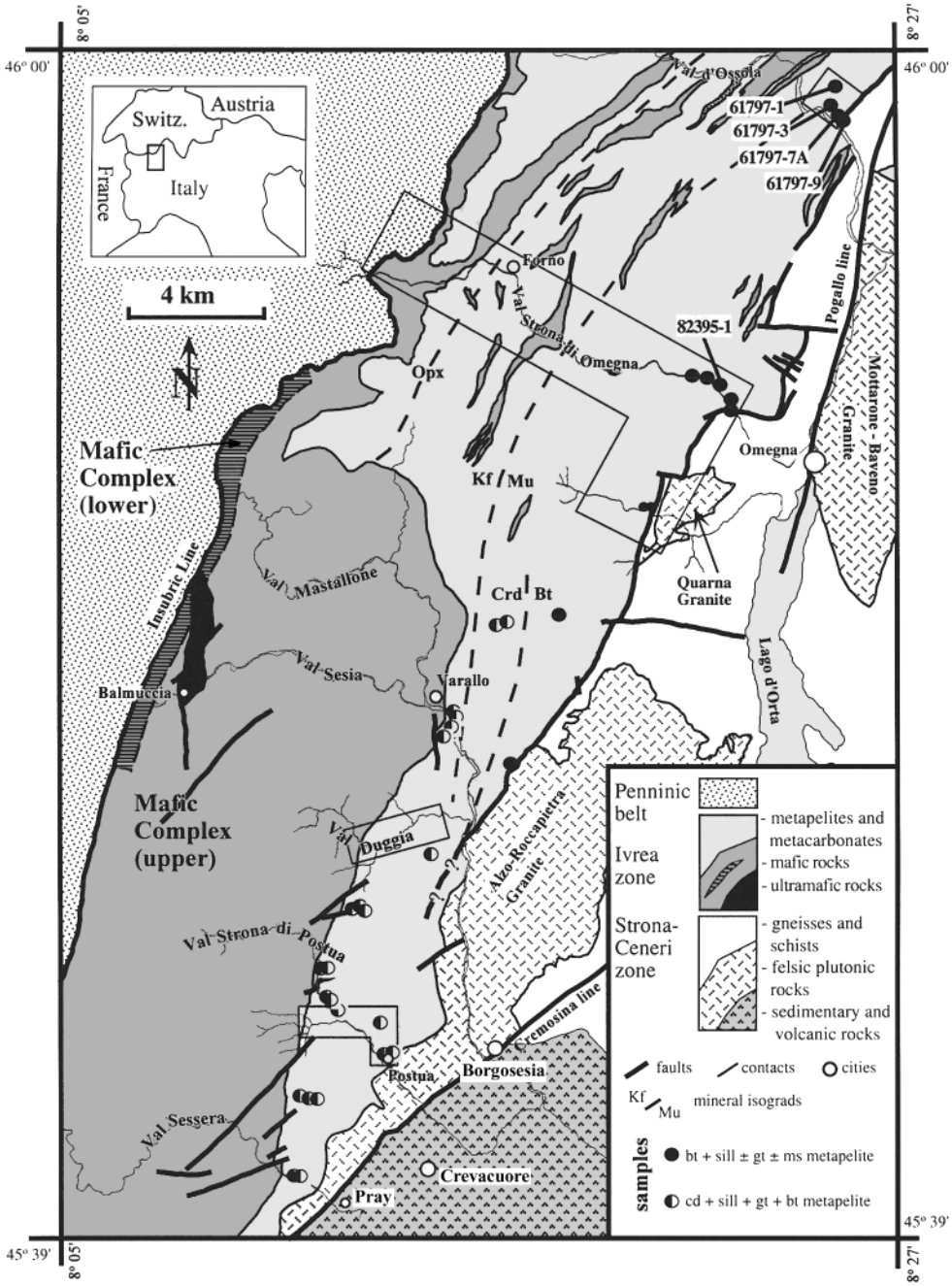

Fig. 1. Geological map of the southern Ivrea and Strona–Ceneri zones west of Lago d'Orta. Inset shows location of study area in northern Italy. Contact between Mafic Complex and Kinzigite Formation based on our own mapping and that reported by Quick *et al.* (1994). Geometry of the boundary between the Ivrea zone and the Strona–Ceneri zone between Val Strona di Omegna and Val d'Ossola taken from Boriani *et al.* (1990*a*). The muscovite–K-feldspar isograd in sillimanite-bearing paragneiss, and the first appearance of orthopyroxene in mafic rocks are indicated by the dashed lines (Schmid, 1967; Zingg, 1980). Enclosed areas within the Kinzigite Formation indicate mapping transects along which samples were collected. Detail sample location maps for R. Forcioula and F. Duggia are provided in Fig. 2.

thickness of 10 km. In this area, the upper Mafic Complex comprises leucodioritic to gabbroic rocks intercalated with ultramafic rocks and layers of banded granulite (Quick *et al.*, 1994; Sinigoi *et al.*, 1994). On the basis of field and compositional relationships, these researchers interpreted the upper Mafic Complex to have been emplaced during Late Carboniferous–Early Permian extension within the Ivrea zone. Space for the Mafic

Complex may have been partially accommodated by northward transport and ductile attenuation of the overlying Kinzigite Formation (Quick *et al.*, 1994; Snoke *et al.*, 1999). South of Val Sesia, lensoidal bodies of tonalite to granodiorite diatexite ≤ 200 m thick, which contain blocks and schlieren of metabasite and metapelite, separate the Mafic Complex from the overlying Kinzigite Formation (Bürgi & Klötzli, 1990; Quick *et al.*, 1994). Phase relations and *PT* estimates indicate that emplacement of the Mafic Complex occurred at crustal depths from 4–5 kbar to 8–10 kbar (Demarchi *et al.*, 1998).

Kinzigite Formation

The Kinzigite Formation comprises amphibolite-to-granulite facies metapelite and metapsammite, with subordinate metacarbonate and metabasite. Metabasite south of Val Sesia (Fig. 1) occurs as 25 cm–50 m thick, foliation-parallel lenses or layers intercalated with metapelite and minor metacarbonate. In Val d'Ossola and Val Strona di Omegna, metabasite is more common and thick layers of metabasite and metapelite alternate (Schmid, 1967; Zingg, 1980; Sills & Tarney, 1984). In amphibolite facies rocks, metabasite contains nematoblastic amphibole + plagioclase $\pm$ clinopyroxene. Orthopyroxene appears in granoblastic amphibole- and plagioclase-bearing metabasite with the transition to the granulite facies. Metacarbonate occurs in lenses and bands ≤ 40m thick, which contain a variety of mineral assemblages (Schmid, 1967; Zingg, 1980).

The most common lithology of supracrustal rock is high-Al migmatitic metapelite with sillimanite as the stable aluminosilicate polymorph. In lower Val Strona di Omegna, metapelite commonly contains biotite + quartz + plagioclase $\pm$ garnet $\pm$ sillimanite $\pm$ muscovite $\pm$ K-feldspar. Primary muscovite is restricted to the lowest grade rocks in lower Val Strona di Omegna and Val d'Ossola. Toward the NW, in upper Val Strona di Omegna, the modal proportions of garnet and K-feldspar increase at the expense of biotite and muscovite (Schmid & Wood, 1976; Schmid, 1978–1979). With the exception of rare occurrences in lowermost Val Strona di Omegna (Zingg, 1980) and Val d'Ossola (Peyronel Pagliani & Boriani, 1967), cordierite and hercynitic spinel are restricted to metapelite proximal to the contact with the upper Mafic Complex (Fig. 1). In agreement with Sills (1984), we observed orthopyroxene with garnet, biotite, and plagioclase in one Mg-rich and Al-poor metapelite. Common accessory minerals include rutile, ilmenite, zircon, graphite, apatite, monazite, pyrite, chalcopyrite, and corundum.

Geochronology

Geochronology indicates a Late Carboniferous–Early Permian crystallization age for the upper Mafic Complex. Pin (1986) reported six fractions of nearly concordant zircon U–Pb data with an upper intercept of 285 + 7/–5 Ma from a diorite sample from the upper Mafic Complex. A Carboniferous–Early Permian age for emplacement is supported by Sm–Nd mineral isochrons and a whole-rock Rb–Sr age (Bürgi & Klötzli, 1990; Voshage *et al.*, 1990). Microanalytic U/Pb ages of newly grown zircon within two minor members of the lower Mafic Complex are 299 $\pm$ 5 Ma (Vavra *et al.*, 1999).

The imposition of the regional metamorphic zonation probably occurred within 20 My of emplacement of the upper Mafic Complex (see Hunziker & Zingg, 1980). Vavra *et al.* (1996, 1999) suggested regional granulite facies metamorphism occurred in a single event before 299 $\pm$ 5 Ma, on the basis of an ion microprobe study of zircons from granulite within the lower Mafic Complex and from supracrustal rocks in upper Val Strona di Omegna. A Late Carboniferous age for the regional granulite facies metamorphism is consistent with U–Pb ages on monazite (Köppel, 1974; Henk *et al.*, 1997) and the inferred age of lead loss of 99% (granulite facies rocks) to 85% (amphibolite facies rocks) from discordant zircon populations (Köppel & Grünfelder, 1971; Köppel, 1974). These studies indicate regional metamorphism before 275 $\pm$ 2 Ma (Köppel, 1974), 292 $\pm$ 2 Ma (Henk *et al.*, 1997), and 285 $\pm$ 10 Ma (Köppel & Grünfelder, 1971; Köppel, 1974), respectively, and may reflect cooling below 600°C (monazite) and conditions close to thermal peak (zircon). Although Henk *et al.* (1997) and Vavra & Schaltegger (1999) differed in their interpretation of decreasing monazite ages from 292 $\pm$ 2 Ma near the Pogallo Line to 276 $\pm$ 2 Ma near the Insubric Line, both studies support a Late Carboniferous age for the regional thermal peak of metamorphism.

RESULTS

Sample suite

To constrain the relationship between emplacement of the upper Mafic Complex and the regional metamorphic *PTt* history of the Ivrea zone, we collected samples for petrographic study and geochemical analyses on four traverses across the regional metamorphic zonation through the Kinzigite Formation (Fig. 1). Sample locations were selected from our mapping of the supracrustal section overlying the upper Mafic Complex south of Val Sesia and the maps of Bertolani (1959–1965) and Schmid (1967) for Val Strona di Omegna and Val d'Ossola, respectively. We compared whole-rock major- and trace-element compositions, metamorphic reaction textures,

and mineral compositions in samples collected south of Val Sesia (proximal to the upper Mafic Complex) with more distal samples collected in lower Val Strona di Omegna and Val d'Ossola. Sample locations are indicated in Figs 1 and 2.

Whole-rock geochemistry

Analytical techniques

The migmatites were separated for analysis by first sawing the sample into slabs of leucosome and melanosome. A representative split of 100–500 g of powdered melanosome sample was then taken for X-ray fluorescence (XRF) analysis. Major and trace elements were analyzed using a Philips PW 1404 XRF spectrometer. Corrections were based on a calibration using 40 international standards according to procedures described by Franzini *et al.* (1975) and Leoni & Saitta (1975). The detection limits are 0·01% for major elements and 10 ppm for trace elements. Analytical uncertainties are $\pm 1\%$ of the value for major elements, except for Mg and Na, for which they are $\pm 5\%$. Analytical uncertainties of trace-element analyses are ± 5–10 ppm for the concentrations at ~ 100 ppm and ± 10–20 ppm for those at 30–50 ppm.

Results

New whole-rock, and major- and trace-element compositions of selected metapelite melanosomes are listed in Table 1. Locations for these selected samples are indicated in Figs 1 and 2. Whole-rock compositions projected from muscovite (Val d'Ossola samples) and K-feldspar (F. Duggia and R. Forcioula samples) are depicted in Fig. 3. AFM projections of melanosome compositions indicate that some samples are enriched in Al over Fe and Mg relative to typical high-Al metapelites. Mass balance calculations indicate a systematic depletion of SiO_2, the alkalis, and incompatible trace elements in melanosomes overlying the upper Mafic Complex relative to lower-grade metapelites in lower Val d'Ossola and Val Strona di Omegna (Barboza, 1998). Leucosome adjacent to the melanosome samples collected within Kinzigite Formation overlying the upper Mafic Complex typically are tonalitic in composition, lack mafic phases, and are depleted in K_2O relative to the inferred melt extracted from the melanosomes (Barboza, 1998; Barboza *et al.*, 1999). Banded granulite intercalated with the lower Mafic Complex and exposed in upper Val Strona di Omegna and Val d'Ossola are depleted in incompatible elements and enriched in compatible elements relative to their amphibolite facies equivalents (Sighinolfi & Gorgoni, 1978; Schnetger, 1994; Barboza *et al.*, 1999).

Inferred reaction sequence

Between upper and lower Val Strona di Omegna and Val d'Ossola

The increase in metamorphic grade to the NW in Val Strona di Omegna and Val d'Ossola with increasing original crustal depth characterizes the regional amphibolite to granulite facies metamorphism in the Ivrea zone. We present new data and review the relevant mineralogy and regional reaction textures for comparison with rocks proximal to the upper Mafic Complex only. Interested readers are directed to other studies for a complete analysis and review (Schmid; 1967, 1993; Mehnert, 1975; Schmid & Wood, 1976; Zingg, 1980; Sills, 1984; Zingg *et al.*, 1990; Henk *et al.*, 1997).

On the basis of a compilation of previous petrographic work, Zingg (1980) located mineral isograds that represent prograde reactions produced during the high-grade, regional metamorphic episode (Fig. 1). These isograds include the muscovite–K-feldspar isograd in sillimanite-bearing metapelite, the first appearance of coexisting pyroxenes in metabasite, and the upper stability limit of calcite–quartz–actinolite in calcsilicate. A textural change in metapelite attends the replacement of lepidoblastic muscovite and biotite by granoblastic K-feldspar and garnet with increasing grade (Schmid, 1967; Schmid & Wood, 1976; Hunziker & Zingg, 1980). In the granulite facies rocks of upper Val Strona di Omegna and Val d'Ossola, quartz + hypersthene $\pm$ garnet granulite and calcsilicate are interlayered with granoblastic graphite + sillimanite + garnet gneiss, interpreted to be residua from the melting of metapelite (Schmid & Wood, 1976; Sighinolfi & Gorgoni, 1978; Schmid, 1978–1979; Schnetger, 1994). Schmid & Wood (1976) attributed the progressive increase in modal garnet at the expense of biotite to the continuous reaction

$$\text{biotite} + \text{sillimanite} + \text{quartz} \Rightarrow \text{garnet} + \text{K-feldspar} + \text{rutile} + H_2O \quad (1)$$

Two phases of muscovite growth are apparent SE of the muscovite-out isograd (Fig. 1) in lower Val Strona di Omegna and Val d'Ossola. Muscovite_2 is distinguished from muscovite_1 in that its long axis is oblique to the foliation defined by muscovite_1, biotite, and sillimanite (Fig. 4a). This relationship suggests that muscovite_2 may have appeared during retrograde cooling and hydration through the reaction

$$\text{sillimanite} + \text{K-feldspar} + H_2O \Rightarrow \text{muscovite} + \text{quartz} \quad (2)$$

an inference supported by common textures indicating the direct replacement of sillimanite + K-feldspar by symplectitic intergrowths of muscovite_2 + quartz.

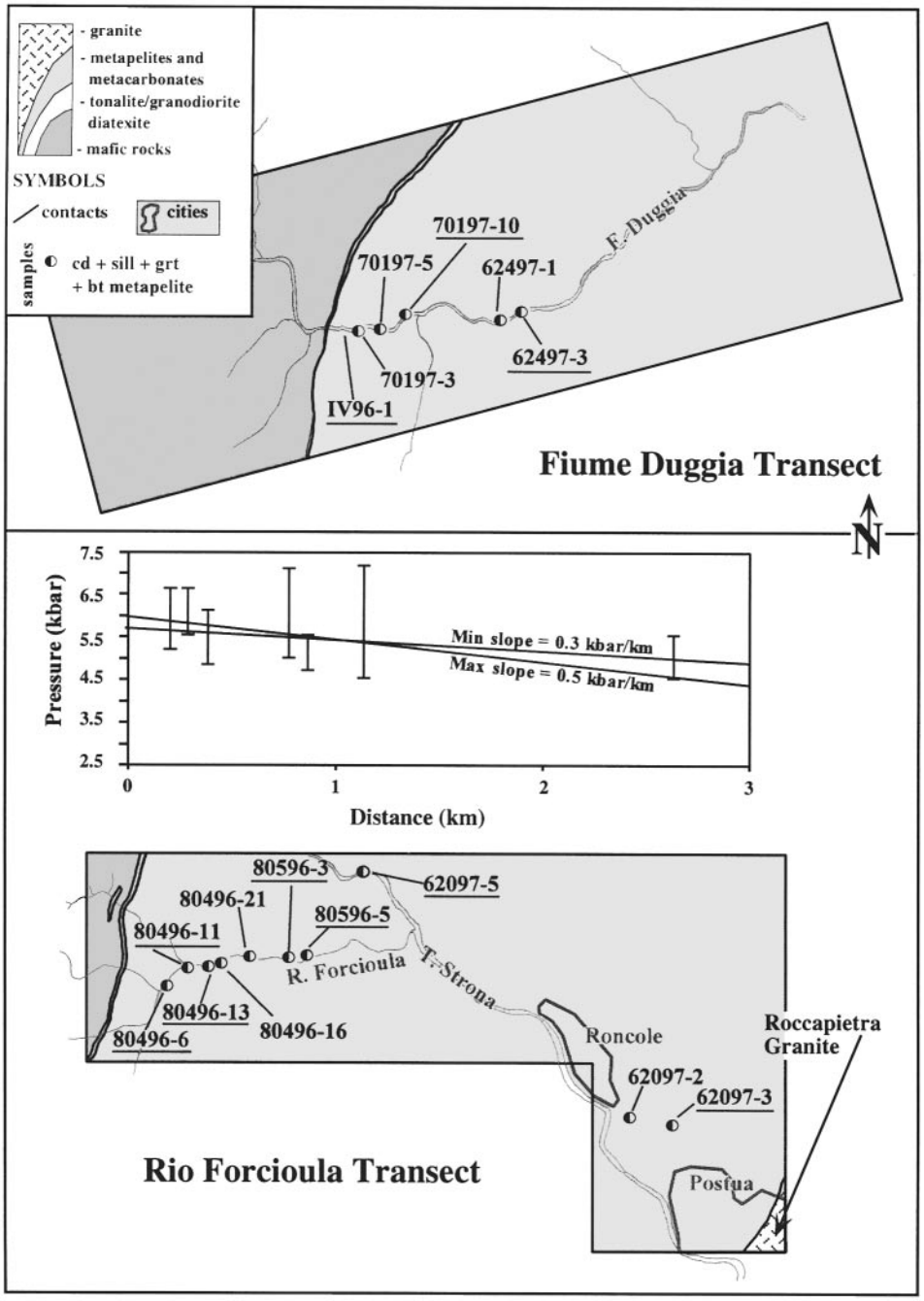

Fig. 2. Detail sample location maps along R. Forcioula and F. Duggia (see Fig. 1). Underlined sample numbers indicate samples used for thermobarometry. Across-strike baric gradient along the R. Forcioula transect with distance from the contact between the Kinzigite Formation and the upper Mafic Complex is also shown.

Between lower Val Sesia and Val Strona di Postua

The longest sections of continuous exposure south of Val Sesia that extend across the contact between the Kinzigite Formation and the upper Mafic Complex are along Rio Forcioula in Val Strona di Postua and Fiume Duggia in Val Duggia (Figs 1 and 2). Mineral assemblages for selected samples collected along these transects are listed in Table 2. Metamorphic grade increases to the SW from the amphibolite facies in lower Val Strona di Omegna, parallel to the regional fabric toward Val

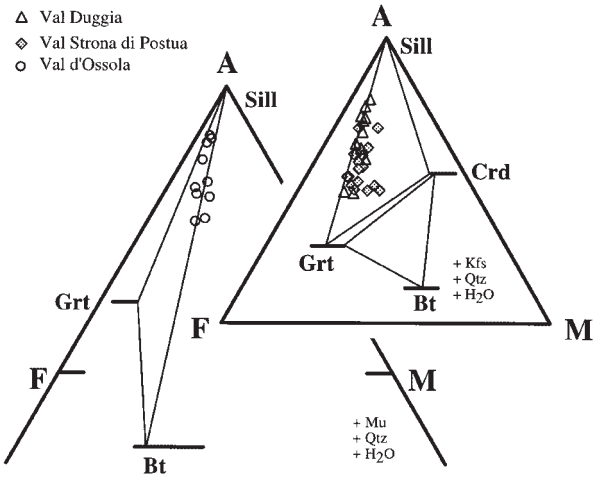

Fig. 3. AFM projection from muscovite (Val d'Ossola samples) and K-feldspar (F. Duggia and R. Forcioula samples) of the whole-rock compositions of metapelites (Table 1). The discontinuous reaction Bt + Sill = Grt + Crd is indicated by the appearance of cordierite within metapelite proximal to the upper Mafic Complex.

Sesia. In the Kinzigite Formation south of Val Sesia, orthopyroxene commonly coexists with plagioclase in amphibole-bearing metabasites, indicating final equilibration of these rocks in the granulite facies.

Zingg (1980) reported the local presence of relict staurolite grains enclosed by cordierite. Relict kyanite has also been reported in two localities south of Val Sesia (Bertolani, 1959; Boriani & Sacchi, 1973), one locality in Val Sesia (Demarchi *et al.*, 1998), and one locality in Val Mastallone (Capedri, 1971). Fibrolite is the dominant textural variety of sillimanite but, with increasing grade, coarse-grained prismatic sillimanite is common. Fibrolite commonly occurs on basal sections of biotite, a texture we associate with the nucleation and growth of sillimanite on biotite indicating the breakdown of staurolite within the stability field of sillimanite (Fig. 4a). The reactions

$$\text{kyanite} \Rightarrow \text{sillimanite} \quad (3)$$

followed by

$$\text{staurolite} + \text{quartz} + \text{muscovite} \Rightarrow \text{garnet} + \text{biotite} + \text{sillimanite} + H_2O \quad (4)$$

probably document the prograde transition from the kyanite + staurolite to the sillimanite stability field.

The muscovite-out isograd in metapelite lies to the NE of the Val Sesia region (Fig. 1), so the limits of muscovite stability were exceeded within the stability field of sillimanite. Accordingly, metapelite that overlies the upper Mafic Complex contains sillimanite + K-feldspar, but lacks primary muscovite (Zingg, 1980). These observations imply the reaction

$$\text{muscovite} + \text{quartz} \Rightarrow \text{sillimanite} + \text{K-feldspar} + H_2O \quad (5)$$

or an H_2O-conserved melting reaction such as

$$\text{muscovite} + \text{plagioclase} + \text{K-feldspar} + \text{quartz} \Rightarrow \text{sillimanite} + \text{melt}. \quad (6)$$

At pressures below 6 kbar, either reaction (5) or (6) in intermediate X_{Mg} metapelite indicates that temperatures proximal to the contact between the upper Mafic Complex and the Kinzigite Formation exceeded ~600°C (Vielzeuf & Holloway, 1988).

In lower Val Strona di Omegna, biotite is the major mineral in metapelite. However, biotite is irregularly distributed in metapelite overlying the Mafic Complex south of Val Sesia: some samples contain <5% modal biotite. The decrease in modal biotite to the SW is coincident with the appearance of abundant cordierite in an ~2–3 km wide aureole overlying the upper Mafic Complex (Fig. 1). We interpret these relationships to indicate that rocks proximal to the eastern magmatic contact with the upper Mafic Complex south of Val Strona di Omegna reached final equilibration within the stability field of cordierite. AFM projections of the bulk compositions of metapelite melanosome (Fig. 3) illustrate the change from the three-phase field defined by garnet–biotite–sillimanite in lower Val Strona di Omegna to garnet–cordierite–sillimanite south of Val Sesia.

Cordierite is typically heavily pinitized, but, when preserved, at least two generations are present (Capedri & Rivalenti, 1973). Cordierite$_1$, found in minor amounts, encloses fibrolite and is elongate parallel to the foliation defined by biotite, sillimanite, and the long axes of garnet augen. This observation implies that cordierite$_1$ growth followed reaction (4). We infer that cordierite$_1$ may have formed from the continuous reaction

$$\text{garnet} + \text{sillimanite} + \text{quartz} \Rightarrow \text{cordierite}_1. \quad (7)$$

The more abundant cordierite$_2$ occurs as up to 5 mm prisms that cut the foliation defined by biotite and sillimanite (Capedri & Rivalenti, 1973). Idiomorphic cordierite$_2$ is present in leucotonalite leucosomes (Barboza *et al.*, 1999) within migmatitic metapelite and occurs abundantly with K-feldspar porphryoblasts in the tonalite to granodiorite diatexite (Bürgi & Klötzli, 1990; Quick *et al.*, 1994) separating the upper Mafic Complex from the overlying Kinzigite Formation south of Val Sesia. These K-poor leucosomes are restricted to the 2–3 km wide aureole that surrounds the upper Mafic Complex, coincident with the appearance of cordierite and hercynitic spinel in the melanosome assemblage. These relationships indicate that cordierite$_2$ was a peritectic phase produced during the melting reaction from which the leucotonalite leucosomes were derived.

Table 1: Whole rock major- and trace-element compositions of representative metapelite melanosomes

Sample	80496	80496	80496	80496	80596	80596	62097	62097	70197	70197	70197	62497	62497	61797	61797	61797	61797	82395
no.:	-11	-13	-16	-21	-03	-05	-05	-02	-03	-05	-10	-01	-03	-01	-03	-07A	-09	-01
Location	RF	RF	RF	RF	RF	RF	RF	RF	VD	VD	VD	VD	VD	VDO	VDO	VDO	VDO	VSO
Major oxide abundances by X-ray fluorescence analysis (wt %)																		
SiO_2	54·72	47·22	46·49	42·37	42·33	38·68	41·78	52·72	53·75	59·5	61·61	55·41	41·78	58·58	57·96	54·86	46·87	53·80
TiO_2	1·75	1·82	1·98	2·59	2·13	2·58	2·31	1·65	1·65	1·34	1·31	1·43	2·31	1·40	1·04	1·21	1·62	0·96
Al_2O_3	20·52	23·63	30·8	29·29	20·77	24·93	32·38	25·32	22·62	20·24	17·30	23·62	32·38	18·13	21·93	21·83	26·15	19·00
FeO^T	11·21	14·56	13·61	14·75	18·17	18·55	14·28	11·68	12·55	10·79	8·72	10·87	14·28	10·39	8·53	9·32	12·87	12·30
MnO	0·16	0·21	0·16	0·18	0·28	0·21	0·19	0·11	0·09	0·09	0·10	0·13	0·19	0·09	0·22	0·08	0·23	0·77
MgO	4·39	6·19	4·35	5·24	6·91	8·00	4·60	3·6	3·81	3·15	4·26	3·24	4·6	3·12	2·35	2·75	3·50	2·50
CaO	2·40	0·91	0·43	0·54	2·80	0·59	1·06	0·37	0·37	0·37	1·08	0·4	1·06	0·31	0·63	0·39	0·45	1·44
Na_2O	1·31	0·51	0·2	0·14	1·77	0·16	0·66	0·38	0·23	0·22	0·68	0·22	0·66	0·57	1·48	1·43	0·57	1·79
K_2O	1·81	2·71	1·58	1·93	3·14	3·53	1·41	2·48	3·31	2·18	2·97	2·85	1·41	4·40	3·51	4·79	4·14	4·36
P_2O_5	0·10	0·03	0·06	n.d.	0·04	0·03	0·07	0·02	0·05	0·04	0·21	0·05	0·07	0·10	0·14	0·10	0·08	n.d.
Total	98·37	97·79	99·66	97·03	98·34	97·26	98·74	98·33	98·43	97·92	98·24	98·22	98·74	97·09	97·79	96·76	96·48	96·92
Trace element abundances by X-ray fluorescence analysis (ppm)																		
Nb	24	20	24	32	18	24	28	21	22	17	15	18	28	23	16	20	23	38
Zr	252	285	240	300	435	450	329	327	280	237	450	270	329	271	168	242	222	205
Y	44	80	42	40	82	70	53	44	46	42	50	43	53	29	31	31	44	33
Sr	248	146	66	46	342	28	112	88	65	90	84	78	112	53	151	109	87	174
Rb	66	84	44	54	132	164	43	79	154	82	88	149	43	201	154	205	173	203
Ba	715	1120	770	505	1045	1275	348	576	826	544	513	617	348	378	654	551	881	1400
La	n.d.	n.d.	n.d.	n.d.	n.d.	n.d.	155	72	71	60	65	68	155	52	49	54	86	n.d.

n.d., not determined. Location abbreviations: RF, Rio Forcioula; VD, Val Duggia; VDO, Val d'Ossola; VSO, Val Strona di Omegna.

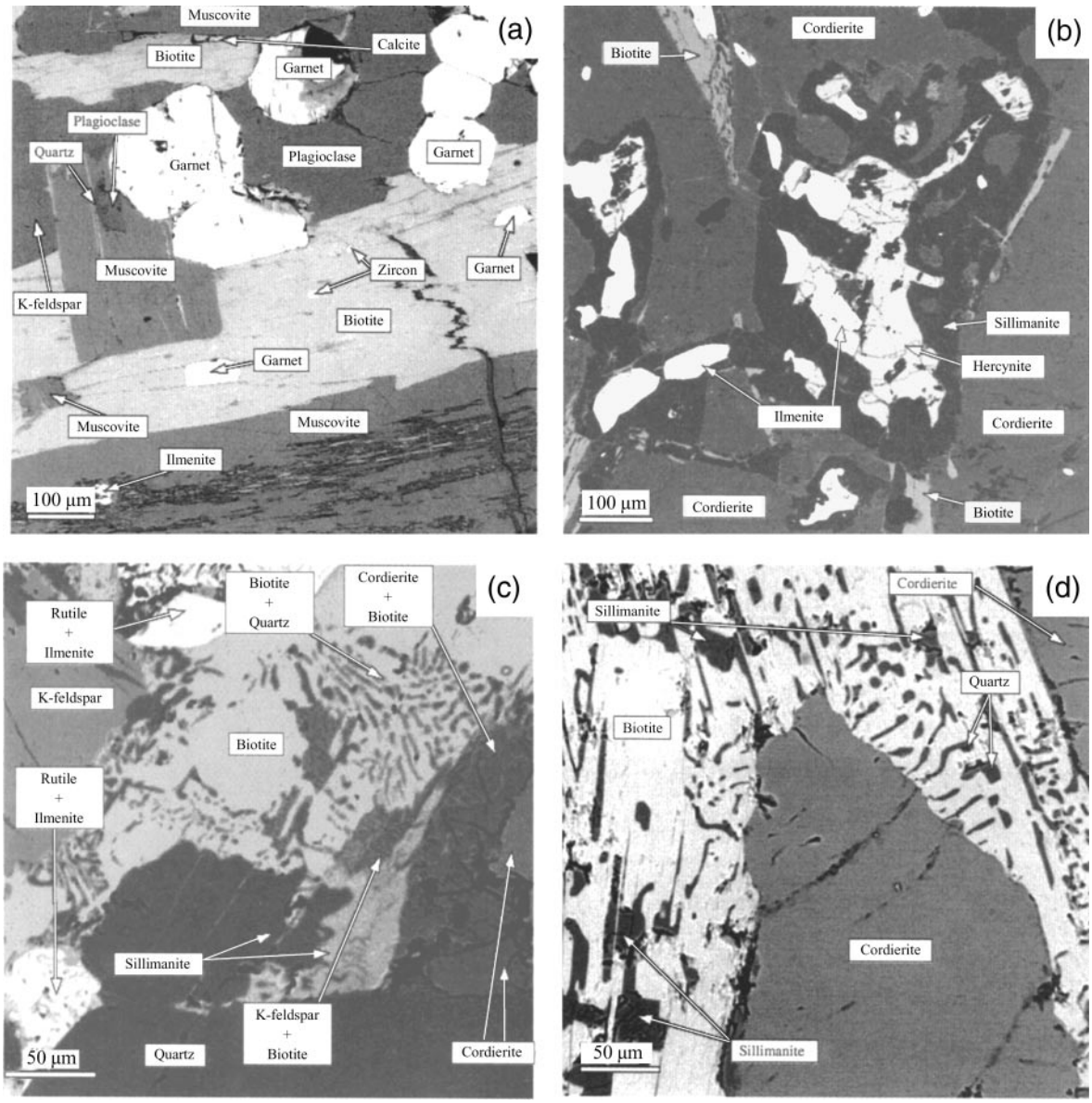

Fig. 4. Electron microprobe backscatter images of (a) retrograde muscovite$_2$ nearly perpendicular to the foliation defined by muscovite$_1$, biotite, and sillimanite; sillimanite–garnet–biotite schist 82395-1, Val Strona di Omegna; (b) hercynitic spinel and ilmenite with sillimanite corona in cordierite$_2$ core; sillimanite–cordierite–garnet gneiss 80596-5, Val Strona di Posuta; (c) retrograde replacement of cordierite + K-feldspar by symplectitic intergrowths of biotite + sillimanite + quartz; sillimanite–cordierite–garnet gneiss 62097-3; (d) close-up of cordierite$_2$ with reaction rim of radiating biotite + quartz + sillimanite symplectite; sillimanite–cordierite–garnet gneiss 62097-3.

Garnet grains in metapelite from lower Val Strona di Omegna and Val d'Ossola are typically idiomorphic, exhibit interior zoning, and are restricted to <250–300 μm in diameter (Fig. 4a). In contrast, garnet grains proximal to the upper Mafic Complex are typically elongate parallel to the foliation defined by biotite and sillimanite, do not exhibit interior zoning, and exceed 1100 μm in diameter. Coarse-grained garnet augen in metapelite proximal to the upper Mafic Complex commonly exhibit inclusion-rich cores surrounded by inclusion-free rims. We interpret these textural relationships to indicate at least two episodes of garnet growth, the latter of which occurred within the stability field of cordierite. Garnet growth associated with the development of peritectic cordierite implies that the reaction

Table 2: Mineral assemblages

Sample	Location	Qtz	Kf	Plg	Ga	Bi	Sil	Cd	Spi	Rt	Il	Pyr	Mn	Ap	Zr
80496-6	RF	X		X	X	X	X	X			X	X	X		
80496-11	RF	X	X	X	X	X	X	X		X	X	X	X	X	
80496-13	RF	X		X	X	X	X	X		X	X				X
80596-3	RF	X		X	X	X	X	X			X		X		
80596-5	RF	X		X	X	X	X	X	X		X		X		X
62097-5	RF	X		X	X	X	X	X		X	X			X	
62097-3	RF	X	X	X	X	X	X	X		X	X			X	X
IV96-1	VD	X	X	X	X	X	X	X				X			X
70197-10	VD	X	X	X	X	X	X	X			X		X		
62497-3	VD	X		X	X	X	X	X		X	X				X

Location abbreviations as in Table 1 X indicates mineral present in sample.

$$\text{biotite} + \text{sillimanite} + \text{quartz} \Rightarrow \text{garnet} + \text{cordierite}_2 + \text{K-feldspar} + \text{melt} \quad (8)$$

occurred within metapelite restricted to a 2–3 km aureole surrounding the upper Mafic Complex.

Grains of hercynitic spinel with sillimanite corona are occasionally present and are always enclosed within cordierite$_2$ (Fig. 4b). This observation is consistent with the prograde reaction

$$\text{biotite} + \text{sillimanite} \Rightarrow \text{cordierite}_2 + \text{hercynitic spinel} + \text{K-feldspar} + \text{ilmenite}\} + \text{melt} \quad (9)$$

in locally quartz-deficient domains, or the retrograde reaction

$$\text{sillimanite} + \text{melt} \Rightarrow \text{cordierite}_2 + \text{hercynitic spinel}. \quad (10)$$

In agreement with the observations of Capedri & Rivalenti (1973), we observed occasional neoblasts of fine-grained, idiomorphic, inclusion-free garnet, perhaps indicating an episode of post-tectonic garnet growth. Retrograde replacement of the assemblage cordierite$_{1,2}$ + K-feldspar is indicated by the development of symplectitic intergrowths of biotite + sillimanite + quartz (Fig. 4c and d). This observation implies retrograde hydration via reaction with a vapor phase or reaction with residual melt through the equilibrium

$$\text{garnet} + \text{cordierite}_2 + \text{K-feldspar} + \text{H}_2\text{O/melt} \Rightarrow \text{biotite} + \text{sillimanite} + \text{quartz}. \quad (11)$$

Andalusite has been reported between lower Val Sesia and Val Sessera (Capedri & Rivalenti, 1973; Zingg, 1980; Demarchi *et al.*, 1998). The reported abundance of andalusite increases to the SW, and it is common near Biella in Valle Mosso (Bertolani, 1959; Sacchi, 1962). Although Zingg (1980) interpreted andalusite to be a relict phase, Capedri & Rivalenti (1973) inferred that andalusite grew after sillimanite, on the basis of microstructural relationships. This implies a retrograde transition from the sillimanite to the andalusite stability field:

$$\text{sillimanite} \Rightarrow \text{andalusite}. \quad (12)$$

Thermobarometry

The widespread occurrence of metapelite in the Kinzigite Formation provides favorable assemblages for thermobarometric constraints upon the regional *PTt* paths. We obtained pressure and temperature estimates with the GASP (3An ⇒ Grs + 2Als + Qtz) reaction and Fe–Mg exchange between garnet and biotite. Calculations were conducted with both MacPTAX (J. Lieberman, unpublished program, 1991) using a 1991 update of Berman's thermodynamic database (Berman, 1988) and TWQ 2·02 (Berman, 1991). MacPTAX adopts the activity models of Berman (1990) for garnet, McMullin *et al.* (1991) for biotite, and Fuhrman & Lindsley (1988) for plagioclase. TWQ 2·02 adopts the activity models of Berman & Aranovich (1995, 1996) for garnet and biotite, and Fuhrman & Lindsley (1988) for plagioclase. MacPTAX typically returns temperatures and pressures ~50–100°C and ~1–2 kbar lower than TWQ 2·02.

We estimated *PT* conditions for nine samples collected on traverses along the Rio Forcioula (6) and Fiume Duggia (3) (Fig. 2). To estimate 'peak' conditions, we compared garnet core compositions free of local zoning near inclusions (determined by X-ray mapping and microprobe analyses) with plagioclase cores and neighboring matrix biotite not in contact with garnet. Mineral compositions and garnet and plagioclase zoning patterns

Table 3: Representative matrix biotite analyses*

Sample	80496	80496	80496	80596	80596	62097	62097	IV96	70197	62497
no.:	-06	-11	-13	-03	-05	-05	-03	-01	-10	-03
Location	RF	RF	RF	RF	RF	RF	RF	VD	VD	VD
SiO_2	36·78	36·66	36·91	36·76	35·62	36·52	35·34	36·28	36·45	36·28
TiO_2	5·56	5·04	3·94	5·23	4·63	4·28	3·78	4·84	4·45	3·47
Al_2O_3	16·57	16·31	16·59	17·21	16·84	17·66	18·55	17·59	18·11	16·51
FeO^T	13·60	13·08	12·91	14·08	14·15	16·06	19·11	15·39	14·00	15·08
MgO	12·14	13·43	14·33	12·51	13·57	11·96	9·82	11·75	12·37	13·55
Na_2O	0·09	0·05	0·14	0·09	0·40	0·11	0·13	0·10	0·16	0·11
K_2O	9·48	9·83	9·48	9·68	9·80	9·61	9·23	9·80	9·83	9·51
Total	94·22	94·4	94·3	95·56	95·01	96·2	95·96	95·75	95·37	94·51
Si	5·51	5·49	5·51	5·45	5·36	5·42	5·33	5·41	5·41	5·47
Ti	0·63	0·57	0·44	0·58	0·52	0·48	0·43	0·54	0·50	0·39
Al	2·93	2·88	2·92	3·01	2·99	3·09	3·30	3·09	3·17	2·93
Al^{IV}	2·49	2·51	2·49	2·56	2·64	2·58	2·67	2·60	2·59	2·53
Al^{VI}	0·44	0·36	0·43	0·45	0·34	0·51	0·63	0·49	0·58	0·40
Fe	1·57	1·51	1·48	1·60	1·64	1·83	2·22	1·76	1·60	1·75
Mg	2·71	3·00	3·19	2·76	3·04	2·65	2·21	2·61	2·74	3·04
Na	0·03	0·01	0·04	0·02	n.d.	0·03	0·04	0·03	0·05	0·03
K	1·81	1·88	1·80	1·83	1·88	1·82	1·78	1·86	1·86	1·83
X_{Fe}†	0·29	0·28	0·27	0·30	0·30	0·34	0·40	0·33	0·30	0·32
X_{Mg}	0·50	0·56	0·57	0·51	0·55	0·48	0·40	0·48	0·51	0·54
X_{Ti}	0·12	0·10	0·08	0·11	0·09	0·09	0·08	0·10	0·09	0·07
$X_{Al^{VI}}$	0·09	0·07	0·08	0·08	0·06	0·09	0·11	0·09	0·11	0·07

*All mineral analyses obtained using the JEOL 733 electron microprobe at the University of Washington. The term 'representative' indicates that data are actual analyses (not averages) and are characteristic of the sample analyzed.
†Mole fraction $Z = X_Z/(X_{Fe} + X_{Mg} + X_{Ti} + X_{Al^{VI}})$.

were obtained by X-ray mapping and electron microprobe analyses. Guided by the X-ray maps and microprobe transects, we analyzed 3–5 points per mineral and 4–6 inferred near-peak equilibrium mineral combinations (garnet–biotite–plagioclase) per sample. The compositional variability of minerals within a sample results in a range of calculated pressures and temperatures. Sample locations are provided in Fig. 2, and representative mineral analyses are listed in Tables 3–5. In accordance with Guidotti & Dyars' (1991) empirical model, we assumed that ferric iron accounted for 8% of FeO^T in biotite. We assumed $FeO^T = FeO$ in garnet.

The results of the thermobarometric calculations are depicted in Fig. 5 and tabulated in Table 6. Although estimated pressures (~3–6 kbar) and temperatures (650–750°C) are consistent with the mineral assemblages, these conditions probably do not correspond to a local thermal maximum. As a result of retrograde Fe–Mg exchange and the fact that exchange and net transfer equilibria tend to have different closure temperatures (Frost & Chacko, 1989), our calculation of 'peak' conditions should be regarded as a minimum estimate of the *PT* conditions during a local thermal maximum.

High temperatures are also indicated by a change of garnet zoning patterns with proximity to the upper Mafic Complex. South of Val Sesia, the predominant garnets are medium- to coarse-grained augen, elongate parallel to the foliation defined by sillimanite and biotite. At least three phases of garnet growth are evident. Garnet augen consist of inclusion-rich cores, surrounded by inclusion-free rims. Late, fine-grained, inclusion-free, idiomorphic garnet cuts the foliation defined by biotite, sillimanite, and the long axes of garnet augen. Garnet grains from lower Val Strona di Omegna and Val d'Ossola samples are weakly zoned in grossular and, to a lesser extent, spessartine contents with the most extreme zonation being within ~5–10 μm of their rims. In contrast, garnet grains in samples collected south of Val Sesia are virtually

Table 4: Representative garnet core compositions.

Sample	80496	80496	80496	80596	80596	62097	62097	IV96	70197	62497
no.:	-06	-11	-13	-03	-05	-05	-03	-01	-10	-03
Location	RF	RF	RF	RF	RF	RF	RF	VD	VD	VD
SiO_2	38·13	38·44	38·46	38·72	38·16	38·78	37·84	37·96	38·19	38·78
TiO_2	<d.l.	0·02	0·04	<d.l.	0·02	0·02	<d.l.	<d.l.	<d.l.	0·02
Al_2O_3	21·53	21·66	21·26	20·43	21·72	20·23	21·42	21·89	21·71	20·42
FeO^T	30·26	29·68	31·22	30·26	31·75	33·37	34·83	32·34	31·53	32·58
MnO	0·49	0·72	0·62	0·65	0·55	0·46	0·87	0·44	0·74	0·57
MgO	7·66	7·50	7·05	7·48	6·89	5·31	4·29	6·37	6·64	6·69
CaO	1·12	1·52	1·22	1·67	1·29	1·26	1·15	1·12	1·33	1·32
Total	99·19	99·54	99·87	99·21	100·38	99·43	100·4	100·12	100·14	100·38
Si	6·00	6·01	6·03	6·10	5·97	6·17	6·01	5·97	5·99	6·09
Ti	0·00	0·00	0·00	0·00	0·00	0·00	0·00	0·00	0·00	0·00
Al	3·99	3·99	3·93	3·79	4·01	3·79	4·01	4·05	4·01	3·78
Fe	3·98	3·88	4·10	3·99	4·15	4·44	4·63	4·25	4·13	4·28
Mn	0·07	0·10	0·08	0·09	0·07	0·06	0·12	0·06	0·10	0·08
Mg	1·79	1·75	1·65	1·76	1·61	1·26	1·02	1·49	1·55	1·57
Ca	0·19	0·26	0·21	0·28	0·22	0·21	0·20	0·19	0·22	0·22
X_{alm}*	0·66	0·65	0·68	0·65	0·69	0·74	0·78	0·71	0·69	0·70
X_{spe}	0·01	0·02	0·01	0·01	0·01	0·01	0·02	0·01	0·02	0·01
X_{pyr}	0·30	0·29	0·27	0·29	0·27	0·21	0·17	0·25	0·26	0·26
X_{grs}	0·03	0·04	0·03	0·05	0·04	0·04	0·03	0·03	0·04	0·04

<d.l., below detection limit.
*Mole fraction $Z = X_Z/(X_{alm} + X_{spe} + X_{pyr} + X_{grs})$.

unzoned (Barboza, 1998). The absence of compositional zoning within garnet grains from samples overlying the upper Mafic Complex probably indicates that homogenization at temperatures exceeding 600–650°C was followed by rapid cooling (Yardley, 1977; Whitney & Dilek, 1998).

Pressure–temperature history

Petrogenetic grid

Our regional *PTt* path is based on the sequence of metamorphic reactions deduced from microstructural interpretations with additional constraints provided by *PT* estimates derived from geothermobarometry. The petrogenetic grid we used (Fig. 6a) includes the beginning of melting in the system Qz–Ab–An–Or–H_2O (Johannes, 1984) and relevant subsolidus and melting reactions for intermediate X_{Mg} pelites (Vielzeuf & Holloway, 1988) in the system KFMASH. The bulk composition of typical metapelite in the Ivrea zone approximates the intermediate X_{Mg} metapelite for which the grid applies (Fig. 3). For clarity, single lines represent the divariant fields for the equilibria in Fig. 6. The omission of Fe_2O_3, TiO_2, Na_2O, and CaO from the KFMASH model system precludes the consideration of reactions involving Fe–Ti oxides and plagioclase. The inclusion of an albite component shifts melting curves to ~40°C lower temperatures (Vielzeuf & Holloway, 1988); an anorthite component reduces this effect (Thompson & Tracy, 1979; Carrington & Harley, 1995).

Summary of inferred PTt *path*

The thick shaded line in Fig. 6b illustrates *PTt* path 'A', for rocks proximal to the upper Mafic Complex south of Val Sesia. *PTt* path 'B' is for rocks distal to the upper Mafic Complex in Val Strona di Omegna. Both paths were inferred for rocks at the approximate structural level of the contact between the upper Mafic Complex and the Kinzigite Formation south of Val Sesia. Arrows indicate constraints on the *PTt* path for which we interpret microstructural evidence that the indicated reaction boundaries were crossed during metamorphism. *PT* and age constraints obtained from geothermobarometry (Fig. 5) and geochronology are also shown.

Reported occurrences of relict kyanite and staurolite (Bertolani, 1959; Boriani & Sacchi, 1973; Zingg, 1980)

Table 5: Representative matrix plagioclase analyses.

Sample	80496	80496	80496	80596	80596	62097	62097	IV96	70197	62497
no.:	-06	-11	-13	-03	-05	-05	-03	-01	-10	-03
Location	RF	RF	RF	RF	RF	RF	RF	VD	VD	VD
SiO_2	57·64	55·51	58·97	59·72	58·37	58·92	60·41	57·76	56·80	58·57
Al_2O_3	26·04	27·79	25·93	25·36	25·68	26·16	25·15	25·49	27·44	25·54
CaO	7·60	8·58	7·81	7·25	8·42	7·54	6·08	6·68	9·10	7·41
Na_2O	7·35	6·43	6·68	7·12	7·09	6·94	8·11	7·70	6·15	7·23
K_2O	0·21	0·14	0·14	0·26	0·09	0·19	0·12	0·24	0·15	0·14
FeO	n.d.	<d.l.	0·02	<d.l.	n.d.	n.d.	0·08	n.d.	0·08	0·04
Total	98·84	98·45	99·55	99·71	99·65	99·75	99·95	97·87	99·72	98·93
Si	2·61	2·53	2·64	2·67	2·62	2·63	2·55	2·64	2·55	2·64
Al	1·39	1·49	1·37	1·33	1·36	1·34	1·45	1·37	1·45	1·36
Ca	0·37	0·42	0·37	0·35	0·40	0·36	0·44	0·33	0·44	0·36
Na	0·65	0·57	0·58	0·62	0·62	0·63	0·54	0·68	0·54	0·63
K	0·01	0·01	0·01	0·02	0·01	0·01	0·01	0·01	0·01	0·01
Fe	n.d.	0·00	0·00	0·00	n.d.	n.d.	0·00	n.d.	0·00	0·00
X_{an}*	0·36	0·42	0·39	0·35	0·39	0·36	0·45	0·32	0·45	0·36
X_{ab}	0·63	0·57	0·60	0·63	0·60	0·63	0·55	0·67	0·55	0·63
X_{or}	0·01	0·01	0·01	0·02	0·01	0·01	0·01	0·01	0·01	0·01

*Mole fraction $Z = X_Z/(X_{an} + X_{ab} + X_{or})$.

probably document the prograde transition from the kyanite + staurolite to the sillimanite stability field. The trajectory and maximum pressure attained along the early prograde path, however, are unconstrained (Fig. 6b). Microstructural evidence [reactions (5) and (6)] indicates that the regional *PT* conditions entered the stability field of sillimanite before exceeding the limits of muscovite stability, constraining the conditions along this portion of the prograde path to $P < 8$ kbar and $T < 750$–800°C. Additionally, we speculate that the common occurrence of fibrolite on biotite grains indicates that the staurolite-out reaction boundary was also crossed within the stability field field of sillimanite, limiting this portion of the prograde path to $P < 7$ kbar and $T < 700$°C. Together, these observations indicate that moderate pressures prevailed for much of the prograde *PT* evolution of the Ivrea zone. Henk *et al.* (1997) inferred that rocks in lower Val Strona di Omegna reached final equilibration from 4 to 6 kbar and from 650 to 700°C (marked 'I' in Fig. 6b).

The presence of peritectic cordierite$_2$ [reaction (8)] requires that temperatures exceeding 650°C were maintained proximal to the upper Mafic Complex during decompression from the regional thermal maximum. Decompression at lower temperatures leads to the breakdown of biotite producing cordierite in the presence of a vapor phase rather than a melt (Fig. 6a). Temperatures exceeding 650°C at moderate pressures are consistent also with *PT* estimates derived from geothermobarometry (Fig. 5) and with the absence of compositional zoning within garnet in proximal metapelite (Barboza, 1998). Finally, high-grade conditions for rocks proximal to the upper Mafic Complex are consistent with mass-balance calculations that indicate proximal metapelites are depleted by ~20–30% of a granite component relative to counterparts in the lower Val Strona di Omegna (Barboza, 1998). The absence of cordierite and the presence of retrograde muscovite$_2$ [reaction (2)] in metapelite from lower Val Strona di Omegna requires that cooling in rocks distal to the upper Mafic Complex accompanied decompression from the regional baric gradient at the thermal maximum. These observations indicate that the upper Mafic Complex provided the heat to reset local mineral assemblages during decompression from the baric gradient at the regional thermal maximum. Mineral assemblages in rocks more distal to the upper Mafic Complex were incompletely reset and preserve evidence of the pre-existing regional metamorphic zonation.

The predominant microstructural feature of retrograde metamorphism that is preserved in metapelite proximal to the upper Mafic Complex is the replacement of cordierite and K-feldspar by symplectitic intergrowths of biotite + sillimanite + quartz [reaction (10)]. The dP/dT slope (Fig. 6a) of this equilibrium is shallow (Vielzeuf

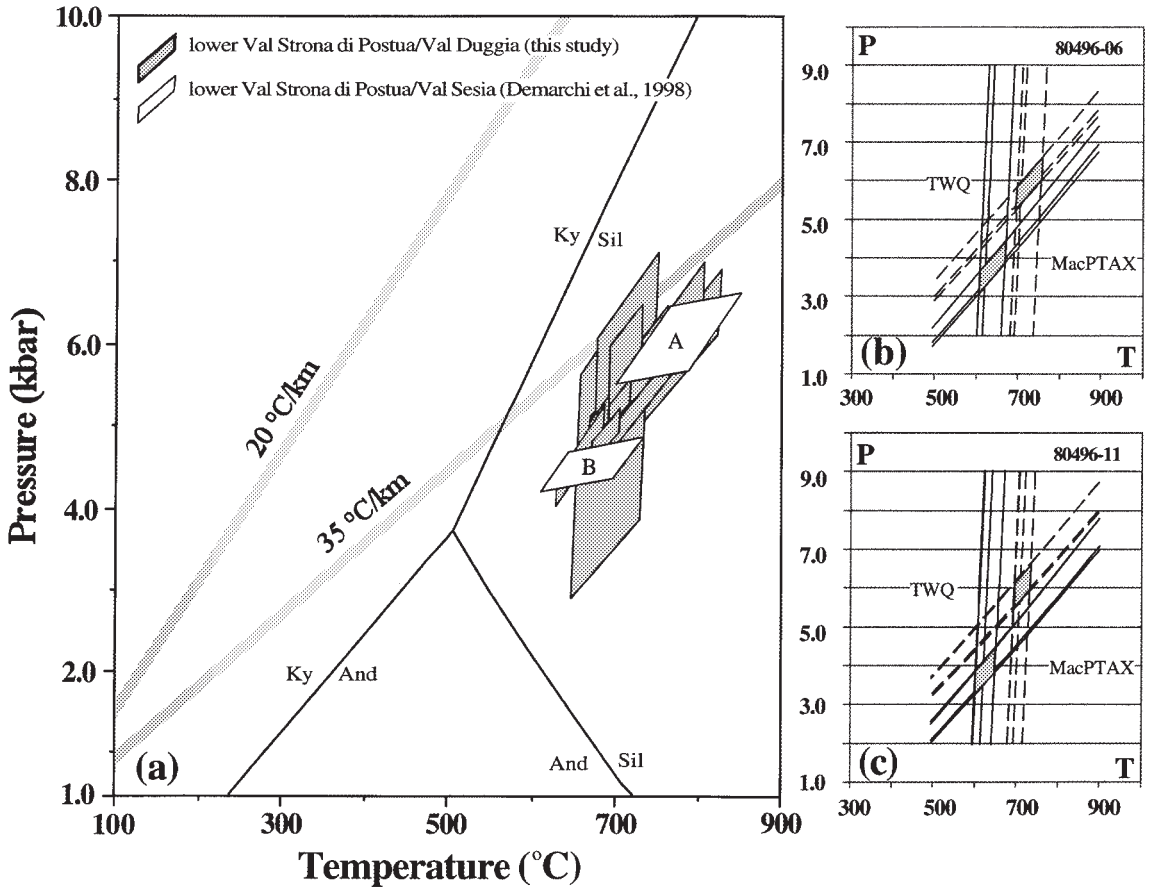

Fig. 5. (a) Shaded polygons depict the results of our thermobarometric calculations (TWQ 2·02) for metapelite overlying the upper Mafic Complex. Dimensions of the polygons determined by the compositional range of each sample. The results of the TWQ 2·02 calculations correlate with the results of Demarchi *et al.* (1998). The results of their study are summarized by the unfilled polygons that enclose the intersections of GASP and garnet–cordierite equilibria with $P_{H_2O} = P_{total}$ (a) and $P_{H_2O} = 0$ (b) calculated for metapelite overlying the upper Mafic Complex (Demarchi *et al.*, 1998). Insets (b) and (c) are example calculations for two samples illustrating the difference between the results of the two algorithms. Calculated *PT* positions of thermobarometric equilibria from individual garnet–biotite and garnet–plagioclase pairs bound the shaded regions. Continuous lines indicate MacPTAX calculations; dashed lines indicate TWQ 2·02 calculations. Complete results of MacPTAX and TWQ 2·02 calculations are given in Table 6.

& Holloway, 1988), indicating that the region followed a near-isobaric cooling path after regional retrograde decompression and magmatism (Fig. 6b). The presence of retrograde andalusite [reaction (11)] probably documents a retrograde transition from the sillimanite to the andalusite stability field.

DISCUSSION AND CONCLUSIONS

Timing of regional and contact metamorphism

Previous interpretation

Although Zingg *et al.* (1990), Schmid (1993), and Barboza *et al.* (1999) took an alternative view, most regional studies have presumed or inferred that final emplacement of the upper Mafic Complex caused regional metamorphism (e.g. Schmid & Wood, 1976; Hunziker & Zingg, 1980; Sills, 1984; Bürgi & Klötzli, 1990; Schnetger, 1994; Sinigoi *et al.*, 1996). This interpretation is based on geochronology, an inferred temperature gradient across the southeastern margin of the upper Mafic Complex (Schmid & Wood, 1976), and a textural gradation from hypidiomorphic–granular to granoblastic with increasing original depth within the upper Mafic Complex (Rivalenti *et al.*, 1980; Quick *et al.*, 1994). Rivalenti *et al.* (1980) and Pin (1990) suggested that this textural gradation is consistent with cooling subsequent to synmetamorphic intrusion.

However, some *PT* estimates (Sills, 1984) do not indicate a regional temperature gradient with proximity to the upper Mafic Complex. Alternative interpretations for the origin of the textural gradation within the upper Mafic Complex (Zingg *et al.*, 1990; Quick *et al.*, 1994)

Table 6: Calculated metamorphic conditions

Sample	Location	MacPTAX		TWQ 2·02	
		T (°C)	*P* (kbar)	*T* (°C)	*P* (kbar)
80496-06	RF	600–650	3·0–4·5	700–750	5·0–6·5
80496-11	RF	600–650	3·5–4·5	675–725	5·5–6·5
80496-13	RF	550–625	3·0–4·0	650–700	5·0–6·0
80596-03	RF	600–650	3·0–5·0	650–725	5·0–7·0
80596-05	RF	600–650	3·0–4·0	650–700	5·0–5·5
62097-05	RF	650–750	4·0–6·0	650–800	4·5–6·5
62097-03	RF	575–625	3·0–4·0	625–800	4·5–5·5
IV96-01	VD	600–700	3·0–5·0	675–700	5·0–5·5
70197-10	VD	600–775	3·0–5·5	700–825	5·0–7·0
62497-03	VD	565–625	3·0–5·0	650–750	3·5–6·0

Location abbreviations as in Table 1.

obviate the need for a causal relationship between magmatism and regional metamorphism. Other observations directly indicate that emplacement of the upper Mafic Complex occurred late relative to the regional granulite facies episode (Zingg *et al.*, 1990; Barboza *et al.*, 1999). Our interpretation that the low-pressure assemblage proximal to the upper Mafic Complex overprints the prograde regional metamorphic zonation supports the conclusion that the regional thermal maximum preceded emplacement of the upper Mafic Complex.

Tectonic implications

Figure 7 depicts a schematic illustration of our new model for metamorphism and magmatism at the Ivrea zone. The presence of relict kyanite and staurolite may suggest that an early phase of crustal thickening accompanied prograde metamorphism (Fig. 7a). Although not the only interpretation of the early prograde metamorphic evolution of the Ivrea zone (see Zingg, 1983; Pin, 1990; Handy & Zingg, 1991), such a prograde contractional event is consistent with evidence of an early phase of high-pressure metamorphism in the Strona Ceneri zone (Boriani & Villa, 1997).

The ubiquitous presence of metapelite with sillimanite in the matrix and as inclusions within garnet indicates that, subsequent to the early contractional phase of metamorphism, much of the prograde *PTt* path occurred within the stability field of sillimanite. The limits of both muscovite and staurolite stability were probably exceeded within the stability field of sillimanite, further indicating that moderate pressures prevailed along much of the prograde path (<7 kbar). At the regional thermal maximum, *PT* conditions for rocks in lower Val Strona di Omegna were 4·0–6·0 kbar and ~650–700°C (Henk *et al.*, 1997), implying a quasi-steady-state thermal gradient of ~40–60°C/km.

These temperatures are elevated with respect to an average crustal geotherm and may require elevated heat flow through a combination of magmatic accretion, aqueous fluid flow, and/or lithospheric extension (De Yoreo *et al.*, 1991). Stable isotopes, however, indicate limited fluid infiltration (Baker, 1988) and the metamorphism we associate with the emplacement of the upper Mafic Complex overprints the regional metamorphic zonation. We suggest that crustal attenuation through tectonic extension (Fig. 7b and c) could explain the moderate pressures along the prograde *PT* path and the elevated geotherm at the regional thermal maximum. Passive upwelling of the asthenosphere accompanied the extension leading to a steepening of the geotherm, thereby enhancing the lower-crustal heat budget (Furlong & Londe, 1986; De Yoreo *et al.*, 1991) and imposing granulite facies conditions at relatively shallow crustal levels. Lachenbruch & Sass (1978) inferred a geotherm of > ~40°C/km for the Battle Mountain High in the Basin and Range Province, a thermal gradient sufficiently steep to explain the *PT* conditions at the regional thermal maximum at the Ivrea zone (Fig. 5).

Decompression subsequent to the regional thermal maximum is documented by the appearance of a lower-pressure assemblage (cordierite, hercynitic spinel) within depleted metapelite proximal to the upper Mafic Complex. The absence of these phases and the presence of retrograde muscovite$_2$ require that cooling accompanied

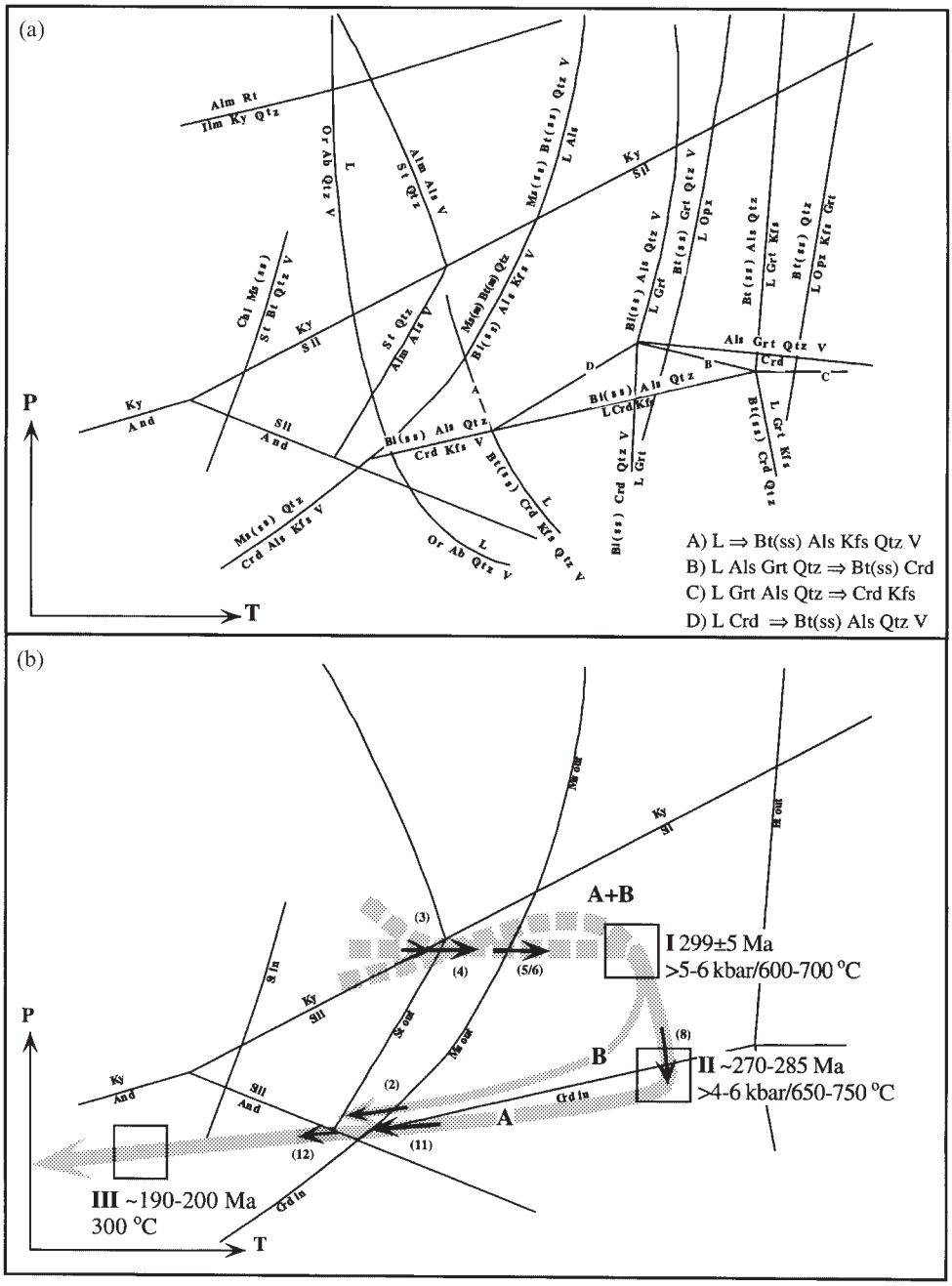

Fig. 6. (a) Partial petrogenetic grid for intermediate X_{Mg} metapelite. Single lines represent divariant fields for clarity. Reaction boundaries adapted after Jones & Brown (1990) and references therein. Reaction Chl + Ms(ss) ⇒ St + Bt + V from Xu *et al.* (1994). (b) Proposed *PTt* path. The two paths represent the *PTt* paths of rocks proximal (path A) and distal (path B) to the upper Mafic Complex. (I), *PT* conditions and age constraints at the regional thermal maximum; (II), thermal maximum for rocks proximal to the upper Mafic Complex discussed in text; (III), cooling age below ~300°C based on K–Ar biotite ages (Bürgi & Klötzli, 1990). Alternative interpretations of the prograde metamorphic evolution reflect the range of uncertainty in the dashed portion of the prograde *PTt* path.

decompression in rocks distal to the upper Mafic Complex. Emplacement of the upper Mafic Complex occurred during retrograde decompression from the regional thermal maximum (Fig. 7c) and provided the thermal energy to reset proximal mineral assemblages. Mineral assemblages in distal rocks were incompletely reset and preserve evidence of higher pressures at the regional thermal maximum (Fig. 5).

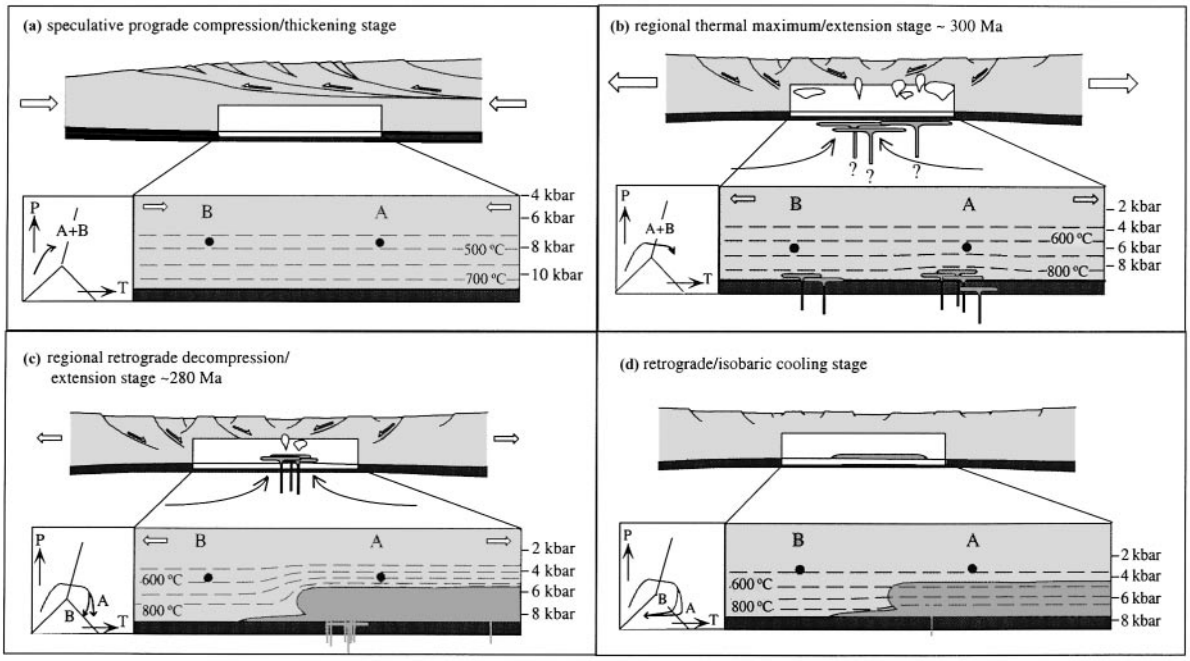

Fig. 7. Inferred tectonic evolution of the Ivrea zone (see text for discussion). As in Fig. 6, points A and B represent rocks at approximately the same crustal level, but situated proximal (A) and distal (B) to the upper Mafic Complex. Placement of the isotherms and isobars is schematic and based on our inferred regional *PTt* path.

We attribute the decompression from the regional baric gradient at the regional thermal maximum to crustal thinning by continued tectonic extension. This interpretation is consistent with other observations in the Ivrea zone. Henk *et al.* (1997) inferred a baric gradient of ~0·41 kbar/km in Val Strona di Omegna. Although the uncertainty in baric gradients calculated from mineral equilibria is large, this estimate exceeds the lithostatic gradient of ~0·3 kbar/km (Burke & Fountain, 1990), suggesting crustal attenuation by a factor of ~1·4 subsequent to the closure temperature of the net transfer reactions from which pressure was estimated. Regional extension is consistent with Brodie & Rutter's (1987) inference that 2 km of E–W-directed attenuation within the lowermost 5 km of the Ivrea zone occurred along mylonitic shear zones. Oriented symplectic intergrowths of orthopyroxene, plagioclase, and spinel in metapelite from upper Val Strona di Omegna support an episode of regional, near-isothermal decompression (Brodie, 1995). Handy (1987) estimated 8–10 km of E–W-directed extension along normal faults near the boundary between the Ivrea and Strona–Ceneri zones. Quick *et al.* (1994) interpreted the arcuate structure of relict magmatic foliation in the upper Mafic Complex as implying emplacement into a zone of active extension, an inference consistent with age estimates for the onset of tectonic extension along the regional retrograde *PTt* path (Brodie *et al.*, 1989). Finally, Snoke *et al.* (1999) reported evidence supporting progressive, non-coaxial, ductile deformation within the carapace of supracrustal rocks overlying the upper Mafic Complex, an observation consistent with ductile attenuation through extension during emplacement. Although compositional variability and the thin (~3 km) carapace of Kinzigite Formation overlying the upper Mafic Complex south of Val Sesia preclude a direct calculation of the baric gradient in Val Strona di Postua, significant crustal attenuation can be accommodated by our results (Fig. 2).

We conclude that extension characterized the Ivrea zone from the Late Carboniferous to the Early Permian. The peak thermal episode of regional granulite facies metamorphism resulted from elevated heat flow during extension and was perhaps enhanced by magmatic accretion below the current level of exposure (Henk *et al.*, 1997). Remnants of the prograde and near-peak magmatism that accompanied extension and regional granulite facies metamorphism may be preserved in parts of the lower Mafic Complex (Vavra *et al.*, 1999). Emplacement of the upper Mafic Complex accompanied decompression from ambient pressures at the regional peak of metamorphism during continued extension. The heat released during crystallization of the upper Mafic Complex provided the thermal energy for contact metamorphism up to the granulite facies in proximal crustal

rocks. The occurrence of cordierite, hercynitic spinel, and coarse-grained garnet augen preserves evidence of low-*P*, high-*T* contact metamorphism.

Crustal attenuation after the regional thermal maximum led to decompression melting of metapelite overlying the upper Mafic Complex and its depletion by up to ~30% granite component (Barboza, 1998). The depleted accumulations of cumulate and peritectic mineral phases that document this melting event are probably represented by the abundant leucotonalitic leucosomes intercalated with metapelite within the upper Mafic Complex contact aureole (Barboza, 1998; Barboza *et al.*, 1999; Snoke *et al.*, 1999). Foliation-parallel melt movement and melt segregation to higher crustal levels may have been directed by penetrative deformation within the carapace of supracrustal rocks overlying the upper Mafic Complex (Snoke *et al.*, 1999). Weakly deformed granitic intrusive bodies in the eastern Ivrea zone may represent the mobilized melt extracted from the contact aureole (Snoke *et al.*, 1999). The cessation of extension and high-grade conditions in rocks proximal to the upper Mafic Complex may have coincided with its final emplacement (Demarchi *et al.*, 1998) and was followed by near-isobaric cooling (Fig. 7d) until Tertiary orogenic activity led to emplacement of the Ivrea zone within the upper crust.

Magmatic accretion models

Our field, petrographic, and geochemical evidence implies that anatexis and metamorphism caused by emplacement of the upper Mafic Complex was confined to a ~3 km aureole in supracrustal rocks that overlie the intrusion. Models that rely upon rapid cooling and convective heat transfer during magmatic accretion (Wells, 1980; Campbell & Turner, 1987) overpredict the extent of crustal heating and anatexis we observe in the Ivrea zone. Huppert & Sparks (1988) calculated that emplacement of basaltic magma at 1200°C into crust at 500–850°C would generate a volume of silicic magma roughly 2·0–0·6 times that of the basalt. This amount exceeds the anatexis we have documented within the upper Mafic Complex contact aureole. Even simulations based on a conductive model for heat transfer (Barboza & Bergantz, 1996) overestimate the extent of the contact aureole and degree of partial melting in <0·1 My after the initiation of magmatism.

The discrepancy between the model results and the field observations may be resolved if the thickness of the contact aureole was reduced by incorporation of residual rocks within the underlying upper Mafic Complex (Voshage *et al.*, 1990; Sinigoi *et al.*, 1996) and attenuation through non-coaxial ductile deformation along the roof of the intrusion (Snoke *et al.*, 1999). According to this view, the contact aureole surrounding the upper Mafic Complex represents the thermal equilibration of crustal rocks with heat released during the final stages of emplacement of the upper Mafic Complex. Large-scale regional metamorphism resulting from emplacement, however, is not apparent, demonstrating that the intrusion of large volumes of mafic magma within the lower continental crust may not inexorably imply regional-scale metamorphism and anatexis of crustal rocks. Reference to studies that predict regional granulite facies metamorphism and extensive crustal anatexis are a necessary consequence of magmatic accretion (Wells, 1980; Campbell & Turner, 1987; Wickham, 1987; Huppert & Sparks, 1988) should be tempered by an awareness that such effects are not apparent in the Ivrea zone, often regarded as an important example of such a process.

ACKNOWLEDGEMENTS

Dr J. Quick, Professor S. Sinigoi, Professor M. Brown, Dr L. Burlini, and Professor A. Boriani are thanked for fruitful discussions and logistical support. Informal reviews by Professor B. W. Evans and Dr Quick, and formal reviews by Professors A. W. Snoke, B. R. Frost, R. Schmid, and B. Hacker substantially improved the manuscript. The detailed editorial assistance of Dr Sorena Sorensen is also greatly appreciated. Partial funding for this work was provided by National Science Foundation grant EAR-9508291, and by a Royalty Research Fund grant from the University of Washington.

REFERENCES

Baker, A. J. (1988). Stable isotope evidence for limited fluid infiltration of deep crustal rocks from the Ivrea zone, Italy. *Geology* **16**, 492–495.

Barboza, S. A. (1998). Anatexis and metamorphism during underplating: field and numerical results. Ph.D. Thesis, University of Washington, Seattle.

Barboza, S. A. & Bergantz, G. W. (1996). Dynamic model of dehydration melting motivated by a natural analogue: applications to the Ivrea–Verbano zone, northern Italy. *Transactions of the Royal Society of Edinburgh* **87**, 23–31.

Barboza, S. A., Bergantz, G. W. & Brown, M. (1999). Regional granulite facies metamorphism in the Ivrea zone: is the Mafic Complex the smoking gun or a red herring? *Geology* **27**, 447–450.

Berckhemer, H. (1968). Topographie des 'Ivrea-Körpers' abgeleitet aus seismischen und gravimetrischen Daten. *Schweizerische Mineralogische und Petrographische Mitteilungen* **48**, 695–732.

Bergantz, G. W. & Dawes, R. (1994). Aspects of magma generation and ascent in continental lithosphere. In: Ryan, M. P. (ed.) *Magmatic Systems*. San Diego, CA: Academic Press, pp. 291–317.

Berman, R. G. (1988). Internally-consistent thermodynamic data for minerals in the system Na_2O–K_2O–CaO–MgO–FeO–Fe_2O_3–Al_2O_3–SiO_2–TiO_2–H_2O–CO_2. *Journal of Petrology* **29**, 445–522.

Berman, R. G. (1990). Mixing properties of Ca–Mg–Fe–Mn garnets. *American Mineralogist* **75**, 328–344.

Berman, R. G. (1991). Thermobarometry using multiequilibrium calculations: a new technique with petrologic applications. *Canadian Mineralogist* **29**, 833–885.

Berman, R. G. & Aranovich, L. Y. (1995). Reanalysis of the garnet–clinopyroxene Fe–Mg exchange thermometer. II. Thermodynamic analysis. *Contributions to Mineralogy and Petrology* **119**, 20–42.

Berman, R. G. & Aranovich, L. Y. (1996). Optimized standard state and solution properties of minerals; I, Model calibration for olivine, orthopyroxene, cordierite, garnet, and ilmenite in the system FeO–MgO–CaO–Al_2O_3–TiO_2–SiO_2. *Contributions to Mineralogy and Petrology* **126**, 25–37.

Bertolani, M. (1959). La formazione basica 'Ivrea Verbano' e la sua posizione nel quadro geologico–petrografico della Bassa Valsesia e del Biellese. *Periodico di Mineralogia* **28**, 151–209.

Bertolani, M. (1959–1965). *Carta geo-lithologica della Valle Strona (Novara)*, 1:25 000.

Bohlen, S. R. (1987). Pressure–temperature–time paths and a tectonic model for the evolution of granulites. *Journal of Geology* **95**, 617–632.

Bohlen, S. R. & Lindsley, D. H. (1987). Thermometry and barometry of igneous and metamorphic rocks. *Annual Review of Earth and Planetary Sciences* **15**, 397–420.

Boriani, A. & Sacchi, R. (1973). Geology of the junction between the Ivrea–Verbano and Strona–Ceneri zones (southern Alps). *Memorie degli Istituti di Geologia e Mineralogia dell'Universita di Padova* **28**, 1–35.

Boriani, A. & Villa, I. M. (1997). Geochronology of regional metamorphism in the Ivrea–Verbano zone and Serie dei Laghi, Italian Alps. *Schweizerische Mineralogische und Petrographische Mitteilungen* **77**, 381–401.

Boriani, A., Bigioggero, B. & Origoni Giobbi, E. (1977). Metamorphism, tectonic evolution, and tentative stratigraphy of the 'Serie dei Laghi'-geological map of the Verbania area (northern Italy). *Memorie degli Istituti di Geologia e Mineralogia dell'Universita di Padova* **32**, 1–25.

Boriani, A., Burlini, L. & Sacchi, R. (1990*a*). The Cossato–Mergozzo–Brissago line and the Pogallo line (southern Alps, N-Italy) and their relationships with the late-Hercynian magmatic and metamorphic events. *Tectonophysics* **182**, 91–102.

Boriani, A., Giobbi Origoni, E., Borghi, A. & Caironi, V. (1990*b*). The evolution of the 'Serie Dei Laghi' (Strona–Ceneri and Schisti dei Laghi): the upper component of the Ivrea–Verbano crustal section; Southern Alps, North Italy and Ticino, Switzerland. *Tectonophysics* **182**, 103–118.

Brodie, K. H. (1995). The development of oriented symplectites during deformation. *Journal of Metamorphic Geology* **13**, 499–508.

Brodie, K. H. & Rutter, E. H. (1987). Deep crustal extensional faulting in the Ivrea Zone of northern Italy. *Tectonophysics* **140**, 193–212.

Brodie, K. H., Rex, D. & Rutter, E. H. (1989). On the age of deep crustal extensional faulting in the Ivrea Zone, northern Italy. In: Coward, M. P., Dietrich, D. & Park, R. G. (eds) *Alpine Tectonics. Geological Society, London, Special Publication* **45**, 203–210.

Bürgi, A. & Klötzli, U. (1990). New data on the evolutionary history of the Ivrea zone (northern Italy). *Bulletin of the Swiss Association of Petroleum Geologists and Engineers* **56**, 49–70.

Burke, M. M. & Fountain, D. M. (1990). Seismic properties of rocks from an exposure of extended continental crust—new laboratory measurements from the Ivrea zone. *Tectonophysics* **182**, 119–146.

Campbell, I. H. & Turner, J. S. (1987). A laboratory investigation of assimilation at the top of a basaltic magma chamber. *Journal of Geology* **95**, 155–172.

Capedri, S. (1971). Sulle rocce della formazione basica Ivrea–Verbano. 2. Petrografia delle granuliti e rocce derivate nella Val Mastallone (Vercelli) e loro evoluzione petrogenetica. *Memorie della Società Geologica Italiana* **10**, 277–312.

Capedri, S. & Rivalenti, G. (1973). Metamorphic crystallisations in relation to plastic deformations in a pelitic series (Valle Strona, Vercelli, Italy). *Bollettino della Società Geologica Italiana* **92**, 649–668.

Carrington, D. P. & Harley, S. L. (1995). Partial melting and phase relations in high-grade metapelites: an experimental petrogenetic grid in the KFMASH system. *Contributions to Mineralogy and Petrology* **120**, 270–291.

Demarchi, G., Quick, J. E., Sinigoi, S. & Mayer, A. (1998). Pressure gradient and original orientation of a lower-crustal intrusion in the Ivrea–Verbano zone, northern Italy. *Journal of Geology* **106**, 609–622.

De Yoreo, J. J., Lux, D. R. & Guidotti, C. V. (1991). Thermal modelling in low-pressure/high-temperature metamorphic belts. *Tectonophysics* **188**, 209–238.

Ellis, D. J. (1987). Origin and evolution of granulites in normal and thickened crust. *Geology* **15**, 167–170.

Fountain, D. M. (1976). The Ivrea–Verbano and Strona–Ceneri zones, northern Italy: a cross-section of the continental crust—new evidence from seismic velocities. *Tectonophysics* **33**, 145–165.

Fountain, D. M. (1989). Growth and modification of lower continental crust in extended terrains: the role of extension and magmatic underplating. In: Mereu, R. F., Mueller, S. & Fountain, D. M. (eds) *Properties and Processes of Earth's Lower Crust. Geophysical Monograph, American Geophysical Union* **51**, 287–299.

Franzini, M., Leoni, L. & Saitta, M. (1975). Revisione di una metodologia analitica per fluorescenza-x, basata sull correzione completa degli effetti di matrice. *Rendiconti della Società Italiana di Mineralogia e Petrologia* **31**, 365–378.

Frost, B. R. & Chacko, T. (1989). The granulite uncertainty principle: limitations on thermobarometry in granulites. *Journal of Geology* **97**, 435–450.

Fuhrman, M. L. & Lindsley, D. H. (1988). Ternary feldspar modeling and thermometry. *American Mineralogist* **73**, 201–215.

Furlong, K. P. & Londe, M. D. (1986). Thermal–mechanical consequences of Basin and Range extension. In: Mayer, L. (ed.) *Extensional Tectonics of the Southwestern United States: a Perspective on Processes and Kinematics. Geological Society of America, Special Paper* **208**, 22–30.

Gans, P. B. (1987). An open-system, two-layer crustal stretching model for the eastern Great Basin. *Tectonics* **6**, 1–12.

Gansser, A. (1968). The Insubric Line, a major geotectonic problem. *Schweizerische Mineralogische und Petrographische Mitteilungen* **48**, 123–143.

Giese, P., Reutter, K.-J., Jacobshagen, V. & Nicolich, R. (1982). Explosion seismic crustal studies in the Alpine Mediterranean region and their implications to tectonic processes. In: Berckhemer, H. & Hsü, K. (eds) *Alpine-Mediterranean Geodynamics. American Geophysical Union, Geodynamics Series* **7**, 39–73.

Guidotti, C. V. & Dyar, M. D. (1991). Ferric iron in metamorphic biotite and its petrologic and crystallochemical implications. *American Mineralogist* **76**, 161–175.

Hamilton, W. B. (1981). Crustal evolution by arc magmatism. *Philosophical Transactions of the Royal Society of London, Series A* **301**, 279–291.

Handy, M. R. (1987). The structure, age and kinematics of the Pogallo fault zone; Southern Alps, northwestern Italy. *Eclogae Geologicae Helvetiae* **80**, 593–632.

Handy, M. R. & Zingg, A. (1991). The tectonic and rheological evolution of an attenuated section of the continental crust: Ivrea crustal section, Southern Alps, northwestern Italy and southern Switzerland. *Geological Society of America Bulletin* **103**, 236–253.

Henk, A., Franz, L., Teufel, S. & Oncken, O. (1997). Magmatic underplating, extension, and crustal reequilibration: insights from a cross-section through the Ivrea Zone and Strona–Ceneri Zone, northern Italy. *Journal of Geology* **105**, 367–377.

Hildreth, W. & Moorbath, S. (1988). Crustal contributions to arc magmatism in the Andes of Central Chile. *Contributions to Mineralogy and Petrology* **98**, 455–489.

Hirn, A., Nadir, S., Thouvenot, F., Nicolich, R., Pellis, G., Scarascia, S., Tabacco, I., Castellano, F. & Merlanti, F. (1989). Mapping the Moho of the Western Alps by wide-angle reflection seismics. *Tectonophysics* **162**, 193–202.

Hodges, K. V. & Fountain, D. M. (1984). Pogallo Line, South Alps, northern Italy: an intermediate crustal level, low angle normal fault? *Geology* **12**, 151–155.

Hunziker, J. C. & Zingg, A. (1980). Lower Palaeozoic amphibolite to granulite facies metamorphism in the Ivrea zone (Southern Alps, northern Italy). *Schweizerische Mineralogische und Petrographische Mitteilungen* **60**, 181–213.

Huppert, H. E. & Sparks, R. S. J. (1988). The generation of granitic magmas by intrusion of basalt into continental crust. *Journal of Petrology* **29**, 599–624.

Jarchow, C. M., Thompson, G. A., Catchings, R. D. & Mooney, W. D. (1993). Seismic evidence for active magmatic underplating beneath the Basin and Range Province, western United States. *Journal of Geophysical Research* **98**, 22095–22108.

Johannes, W. (1984). Beginning of melting in the granite system Qz–Or–Ab–An–H_2O. *Contributions to Mineralogy and Petrology* **86**, 264–273.

Jones, K. A. & Bown, M. (1990). High-temperature 'clockwise' *P–T* paths and melting in the development of regional migmatites: an example from southern Brittany, France. *Journal of Metamorphic Geology* **8**, 551–578.

Kay, R. W. & Kay, S. M. (1981). The nature of the lower continental crust: inferences from geophysics, surface geology, and crustal xenoliths. *Reviews in Geophysics* **19**, 271–297.

Köppel, V. (1974). Isotopic U–Pb ages of monazites and zircons from the crust–mantle transition and adjacent units of the Ivrea and Ceneri zones (southern Alps, Italy). *Contributions to Mineralogy and Petrology* **43**, 55–70.

Köppel, V. & Grünfelder, M. (1971). A study of inherited and newly formed zircons from paragneisses and granitised sediments of the Strona–Ceneri zone (Southern Alps). *Schweizerische Mineralogische und Petrographische Mitteilungen* **51**, 385–410.

Lachenbruch, A. H. & Sass, J. H. (1978). Models of an extending lithosphere and heat flow in the Basin and Range province. *Geological Society of America, Memoir* **152**, 209–250.

Leoni, L. & Saitta, M. (1975). X-ray fluorescence analysis of 29 trace elements in rocks and mineral standards. *Rendiconti della Società Italiana di Mineralogia e Petrologia* **32**, 497–510.

Lister, G. S., Etheridge, M. A. & Symonds, P. A. (1986). Detachment faulting and the evolution of passive continental margins. *Geology* **14**, 246–250.

Mareschal, J.-C. & Bergantz, G. B. (1990). Constraints on thermal models of the Basin and Range province. *Tectonophysics* **174**, 137–146.

Marsh, B. D. (1989). On convective style and vigor in sheet-like magma bodies. *Journal of Petrology* **30**, 479–530.

McMullin, D. W. A., Berman, R. G. & Greenwood, H. J. (1991). Calibration of the SGAM thermobarometer for pelitic rocks using data from phase-equilibrium experiments and natural assemblages. *Canadian Mineralogist* **29**, 889–908.

Mehnert, K. (1975). The Ivrea zone, a model of the deep crust. *Neues Jahrbuch für Mineralogie, Abhandlungen* **125**, 156–199.

Mueller, S., Ansorge, J., Egloff, R. & Kissling, E. (1980). A crustal cross section along the Swiss Geotraverse from the Rhinegraben to the Po Plain. *Eclogae Geologicae Helvetiae* **73**, 463–483.

Nicolas, A., Hirn, A., Nicolich, R., Polino, R. & the ECORS-CROP Working Group (1990). Lithospheric wedging in the Western Alps inferred from the ECORS-CROP traverse. *Geology* **18**, 587–590.

Peyronel Pagliani, G. & Boriani, A. (1967). Metamorfismo crescente nelle metamorfiti del 'Massiccio dei Laghi' nella zona bassa Val d'Ossola–Verbania (Novara). *Rendiconti della Società Italiana di Mineralogia e Petrologia* **23**, 351–397.

Pin, C. (1986). Datation U/Pb sur zircons à 285 Ma du complexe gabbro–dioritique du Val Sesia–Val Mastallone et age tardihercynien du metamorphisme granulitique de la zone Ivrea–Verbano (Italie). *Comptes Rendus de l'Académie des Sciences, Série 2* **303**, 827–830.

Pin, C. (1990). Evolution of the lower crust in the Ivrea zone: a model based on isotopic and geochemical data. In: Vielzeuf, D. & Vidal, P. (eds) *Granulites and Crustal Evolution*. Dordrecht: Kluwer, pp. 87–110.

Quick, J. E., Sinigoi, S. & Mayer, A. (1994). Emplacement dynamics of a large mafic intrusion in the lower crust of the Ivrea–Verbano Zone, northern Italy. *Journal of Geophysical Research* **99**, 21559–21573.

Rivalenti, R., Garuti, G. & Rossi, A. (1975). The origin of the Ivrea–Verbano Basic Formation (western Italian Alps)—whole rock geochemistry. *Bollettino della Società Geologica Italiana* **94**, 1149–1186.

Rivalenti, G., Garutti, G., Rossi, A., Siena, F. & Sinigoi, S. (1980). Existence of different peridotite types and of a layered igneous complex in the Ivrea zone of the Western Alps. *Journal of Petrology* **22**, 127–153.

Sacchi, R. (1962). Nuovi data geologici sull tavoletta Valle Mosso. *Bollettino del Servizio Geologica d'Italia* **83**, 51–59.

Schmid, R. (1967). Zur Petrographie und Struktur der Zone Ivrea–Verbano zwischen Valle d'Ossola und Val Grande (Prov. Novara Italien). *Schweizerische Mineralogische und Petrographische Mitteilungen* **47**, 935–1117.

Schmid, R. (1978–1979). Are the metapelites in the Ivrea zone restites? *Memorie degli Istituti di Geologia e Mineralogia dell'Universita di Padova* **33**, 67–69.

Schmid, R. & Wood, B. J. (1976). Phase relationships in granulitic metapelites from the Ivrea–Verbano zone (northern Italy). *Contributions to Mineralogy and Petrology* **54**, 255–279.

Schmid, S. M. (1993). Ivrea zone and adjacent Southern Alpine basement. In: von Raumer, J. F. & Neubauer, F. (eds) *Pre-Mesozoic Geology in the Alps*. Berlin: Springer, pp. 567–583.

Schmid, S. M., Zingg, A. & Handy, M. (1987). The kinematics of movements along the Insubric Line and the emplacement of the Ivrea Zone. *Tectonophysics* **135**, 47–66.

Schnetger, B. (1994). Partial melting during the evolution of the amphibolite-to-granulite-facies gneisses of the Ivrea Zone, northern Italy. *Chemical Geology* **113**, 71–101.

Sighinolfi, G. P. & Gorgoni, C. (1978). Chemical evolution of high-grade metamorphic rocks—anatexis and remotion of material from granulite terrains. *Chemical Geology* **22**, 157–176.

Sills, J. D. (1984). Granulite facies metamorphism in the Ivrea zone, N.W. Italy. *Schweizerische Mineralogische und Petrographische Mitteilungen* **64**, 169–191.

Sills, J. D. & Tarney, J. (1984). Petrogenesis and tectonic significance of amphibolites interlayered with metasedimentary gneisses of the Ivrea zone, Southern Alps, northwest Italy. *Tectonophysics* **107**, 187–208.

Sinigoi, S., Quick, J. E., Clemens-Knott, D., Mayer, A., Dimarchi, G., Mazzucchelli, M., Negrini, L. & Rivalenti, G. (1994). Chemical evolution of a large mafic intrusion in the lower crust, Ivrea–Verbano zone, northern Italy. *Journal of Geophysical Research* **99**, 21575–21590.

Sinigoi, S., Quick, J. E., Mayer, A. & Budahn, J. (1996). Influence of stretching and density contrasts on the chemical evolution of continental magmas: an example from the Ivrea–Verbano zone. *Contributions to Mineralogy and Petrology* **123**, 238–250.

Snoke, A. W., Kalakay, T. J., Quick, J. E. & Sinigoi, S. (1999). Development of a deep-crustal shear zone in response to syntectonic intrusion of mafic magma into the lower crust, Ivrea–Verbano zone, Italy. *Earth and Planetary Science Letters* **166**, 31–45.

Thompson, A. B. & Tracy, R. J. (1979). Model systems for the anatexis of pelitic rocks. II. Facies series melting reactions in the system $CaO–KAlO_2–NaAlO_2–Al_2O_3–H_2O$. *Contributions to Mineralogy and Petrology* **70**, 429–438.

Vavra, G. & Schaltegger, U. (1999). Post-granulite facies monazite growth and rejuvenation during Permian to Lower Jurassic thermal and fluid events in the Ivrea zone (Southern Alps). *Contributions to Mineralogy and Petrology* **134**, 405–414.

Vavra, G., Gebauer, D., Schmid, R. & Compston, W. (1996). Multiple zircon growth and recrystallization during polyphase Late Carboniferous to Triassic metamorphism in granulites of the Ivrea zone (Southern Alps): an ion microprobe (SHRIMP) study. *Contributions to Mineralogy and Petrology* **122**, 337–358.

Vavra, G., Schmid, R. & Gebauer, D. (1999). Internal morphology, habit and U–Th–Pb microanalysis of amphibolite-to-granulite facies zircons: geochronology of the Ivrea Zone (Southern Alps). *Contributions to Mineralogy and Petrology* **134**, 380–404.

Vielzeuf, D. & Holloway, J. R. (1988). Experimental determination of the fluid-absent melting relations in the pelitic system. *Contributions to Mineralogy and Petrology* **98**, 257–276.

Voshage, H., Hofmann, A. W., Mazzucchelli, M., Rivalenti, G., Sinigoi, S., Raczek, I. & Demarchi, G. (1990). Isotopic evidence from the Ivrea Zone for a hybrid lower crust formed by magmatic underplating. *Nature* **347**, 731–736.

Wells, P. R. A. (1980). Thermal models for the magmatic accretion and subsequent metamorphism of continental crust. *Earth and Planetary Science Letters* **46**, 253–265.

Whitney, D. L. & Dilek, Y. (1998). Metamorphism during alpine crustal thickening and extension in Central Anatolia, Turkey: the Nigde Metamorphic Core Complex. *Journal of Petrology* **39**, 1385–1403.

Wickham, S. M. (1987). Crustal anatexis and granite petrogenesis during low-pressure regional metamorphism: the Trois Seigneurs Massif, Pyrenees, France. *Journal of Petrology* **28**, 127–169.

Xu, G., Will, T. M. & Powell, R. (1994). A calculated petrogenetic grid for the system $K_2O–FeO–MgO–Al_2O_3–SiO_2–H_2O$, with particular reference to contact-metamorphosed pelites. *Journal of Metamorphic Geology* **12**, 99–119.

Yardley, B. W. D. (1977). An empirical study of diffusion in garnet. *American Mineralogist* **62**, 793–800.

Zingg, A. (1980). Regional metamorphism in the Ivrea Zone (Southern Alps, N-Italy): field and microscopic investigations. *Schweizerische Mineralogische und Petrographische Mitteilungen* **60**, 153–173.

Zingg, A. (1983). The Ivrea and Strona–Ceneri Zones (southern Alps, Ticino and N. Italy)—a review. *Schweizerische Mineralogische und Petrographische Mitteilungen* **63**, 361–392.

Zingg, A., Handy, M. R., Hunziker, J. C. & Schmid, S. M. (1990). Tectonometamorphic history of the Ivrea Zone and its relationship to the crustal evolution of the Southern Alps. *Tectonophysics* **182**, 169–192.